Evaluating the geogenic CO_2 flux from geothermal areas by analysing Quaternary travertine masses. New data from western Central Italy and review of previous CO_2 flux data.

A. Mancini[1-4]*, F. Frondini[1], E. Capezzuoli[2], E. Galvez Mejia[1], G. Lezzi[1], D. Matarazzi[1], A. Brogi[3], R. Swennen[4].

alessandro.mancini@kuleuven.be
francesco.frondini@unipg.it
enrico.capezzuoli@unifi.it
edugame_10@hotmail.com
gabriele.lezi@libero.it
david.matarazzi@libero.it
andrea.brogi@uniba.it
rudy.swennen@kuleuven.be

[1] Department of Physics and Geology, University of Perugia, Via Pascoli snc, Perugia, 06123, Italy.

[2] Department of Earth Sciences, University of Florence, Via la Pira 4, 50121, Firenze, Italy

[3] Department of Earth and Geoenvironmental Sciences, University of Bari "Aldo Moro", Via Orabona, 4, 70125 Bari, Italy

[4] Department of Geology, Earth and Environmental Sciences, KU Leuven, Celestijnenlaan 200E, 3001 Heverlee, Belgium.

*corresponding author

Alessandro Mancini: alessandro.mancini@kuleuven.be

Declarations of interest: none

Abstract

Quantification of carbon fluxes between solid Earth and its atmosphere is necessary to understand the global geological carbon cycle. Some of the main CO_2 contributors are metamorphism and magmatic-mantle degassing. CO_2 is discharged from active and quiescent volcanoes, fault zones, geothermal systems and CO_2 rich groundwater. Here a new method for the estimation of the geogenic flux of CO_2 from tectonically active regions, based on the volume, composition and age of travertine deposits, is proposed. The method is applied to the travertine deposits of western Central Italy where travertine deposition is driven by degassing of CO_2 charged groundwater.

Results show that the study areas are characterized, since Middle Pleistocene, by diffuse CO_2 degassing processes with time averaged CO_2 fluxes ranging between 1.24 ± 0.12 10^6 mol y^{-1} km^{-2} and 1.38 ± 0.42 10^6 mol y^{-1} km^{-2}. These values are of the same order of magnitude of carbon dioxide fluxes measured by different methods in western central Italy and are higher than the global baseline CO_2 flux from high heat flow regions.

The review of the available $^{234}U/^{230}Th$ and ^{14}C data shows that the CO_2 degassing processes that affects western Central Italy nowadays were already active at least 350 Ka ago, proving that this region is a globally relevant case for the study of Earth degassing.

Considering the widespread occurrence of travertine deposits in tectonically active areas worldwide, the proposed approach can be used as a reliable tool to estimate the CO_2 flux in different geodynamic settings within system Earth.

Key words: Travertines; Quaternary; Carbon Dioxide degassing; western Central Italy.

1. Introduction

A better quantification of the carbon fluxes between solid Earth and Earth's atmosphere is necessary for modelling the carbon cycle over geological times and its future evolution. It also allows to study the connections between atmospheric CO_2 and climate (Kump et al., 2000; Kurschner, 2001). Even if the geologic component of the carbon cycle - 300 Mt/y CO_2 according to Mörner and Etiope (2002); >600 Mt/y CO_2 according to Burton et al. (2013) - operates slowly in comparison to the other parts of the global carbon cycle, such as the anthropogenic component that is currently characterised by a CO_2 flux 50-100 times higher (Gerlach, 2011; IPCC, 2013; Regnier et al., 2013; Le Quéré et al., 2015), in the long term the carbon budget of Earth's atmosphere is largely controlled by the relative fluxes of CO_2 consumed by chemical weathering of silicates vs CO_2 degassed by metamorphism and magmatism (Berner et al., 1983; Berner, 1993, 2004; Kerrick and Caldeira, 1993, 1998). Most of the models of geologic carbon cycle derive the CO_2 degassing rate assuming that the present-day degassing flux is equal to the flux of CO_2 consumed by chemical weathering of silicates (Berner et al., 1983; Lasaga et al., 1985; Berner, 2006). However, this steady state assumption could be inadequate since there are still major uncertainties on the net direction and magnitude of tectonic carbon fluxes from mantle and crust to the atmosphere: therefore, the degassing flux and the CO_2 consumption by weathering should be estimated independently.

Despite the fact that in recent years some authors computed various global estimations of the carbon dioxide degassing rates from igneous and metamorphic activity (Mörner and Etiope, 2002; Burton et al., 2013), the total subaerial lithospheric CO_2 flux is still far from being quantified. Except for the areas of active volcanism, only a few data on diffuse CO_2 degassing from tectonically active areas are available (e.g. Chiodini et al., 2000; Crossey et al., 2009).

The amount of CO_2 released to the atmosphere from active faults, hydrothermal systems, mantle degassing and/or degassing from non-erupting magmas, is potentially of the same order of magnitude, or greater, than the amount directly measured from active volcanoes (Mörner and Etiope, 2002; Burton et al., 2013; Scott and Lindsey, 2016; Frondini et al., 2019), but at present it is not considered by IPCC estimates (IPCC, 2013), because present day estimations of regional CO_2

fluxes in tectonically active areas are very scarce and regionally widely scattered.

A notable exception is Central-southern Italy, which is one of the few regions of the world where detailed mapping and quantification of the CO_2 fluxes have been performed in the last two decades (Chiodini et al., 1999, 2000, 2004; Minissale, 2004). In particular, Chiodini et al. (2000) showed that a large portion of the inorganic carbon dissolved in groundwater circulating in the central Apennines is derived from a deep, mantle-related source. In addition, Chiodini et al. (2004), based on the carbon balance of regional aquifers, produced the first regional map of CO_2 degassing in central and southern Italy, showing that a globally significant amount of deeply derived CO_2 (2.1×10^{11} mol/y) is released by two large areas in western Italy, called by the authors Tuscan Roman Degassing Structure (TRDS) and Campanian Degassing Structure (CDS); the amount of endogenous CO_2 released to the atmosphere through diffuse regional degassing is the main component of the geological CO_2 budget in Italy (Frondini et al., 2018) and is higher than the amount of CO_2 discharged by active volcanoes, as reported by Burton et al. (2013) for the Etna, Stromboli and Vulcano volcanic complex, and volcanoes with hydrothermal activity (Campi Flegrei and Vesuvio; Frondini et al. 2004; Cardellini et al. 2017).

In western Italy, the areas of diffuse degassing are also characterised by focused gas emissions, anomalous heat flux, thermal and mineral springs and active travertine deposition (Chiodini et al., 1999, 2000, 2013; Minissale et al., 2002; Minissale, 2004).

In this region, deposition of travertine (Capezzuoli et al., 2014) is generally driven by degassing of CO_2 charged groundwater circulating in deep carbonate-evaporitic reservoirs (Frondini, 2008; Frondini et al., 2012; Brogi et al., 2016). When high pCO_2 groundwater emerges at springs, it rapidly degases CO_2, due to the lower atmospheric pCO_2, leading to oversaturation with respect to calcite that precipitates according to the following overall reaction:

$$2HCO_3^- + Ca^{++} = CaCO_3 + CO_2 + H_2O \quad (1).$$

The reaction stoichiometry shows that for each mole of calcite precipitated by groundwater, one mole of CO_2 is degassed to the atmosphere. This simple observation suggests that the estimation of the volume of travertine deposits can be used as an indirect measure of the amount of CO_2 degassed during travertine deposition. For example, D'Alessandro et al. (2007), based on the estimated volume of travertines of the S-W flanks of Mt. Etna (Italy), showed that between 10 and 20 Gg/y (2.2-4.5 × 10^9 mol/y) of CO_2 were involved in travertine deposition for a time span of about 20 Ka. If the age of the travertine is also known together with the surface area of the hydrogeological basin feeding the travertine-depositing springs, it is possible to compute both the cumulative amount of CO_2 degassed during travertine deposition and the time averaged flux of carbon dioxide per unit area. The latter parameter could be very useful both to compare the CO_2 fluxes from different regions and to compare past and present-day carbon dioxide fluxes within the same region.

In this work, we analyze three of the most notable travertine outcrops, deposited in a similar time range (Pleistocene-Holocene), in western central Italy: i.e. Rapolano Terme, Canino and Tivoli (Fig. 1).

The objectives of the study are: (i) to quantify the travertine volume within each area, (ii) to compute the amount of CO_2 degassed related to travertine deposition and (iii) to compare the paleo CO_2 fluxes to the present-day CO_2 flux of the regions. All the considered travertine deposits are related to large thermal spring systems where travertine deposition is still active or was recently active and for all the systems the ages of the travertine deposits are known. Given these characteristics and considering their large extent and thickness, these travertine deposits can act as examples of some of the largest travertine occurrences in the world.

2. Overall geological setting

The travertine masses are located in the western side of the Northern Apennines (Fig. 1), a collisional belt derived from the progressive convergence and collision of the European continental margin (Corsica-Sardinia block) and the Adriatic promontory (Adria) being part of the African plate (Patacca et al., 1992; Carmignani et al., 1994; Molli, 2008; Carminati and Doglioni, 2012; Rossetti et al., 2015). The inner zone of the orogen (i.e. the hinterland) developed through several tectonic phases, mostly during the Cretaceous-Early Miocene, which gave rise to a tectonic pile formed by units belonging to different paleo-geographic domains (Carmignani et al., 1994). The orogenic wedge comprises tectonic units deriving both from oceanic and continental domains of the African paleomargin (Bianco et al., 2015 with references therein). In more detail, the stacked tectonic units are: (a) the Ligurian Units, consisting of several slices made by fragments of Jurassic oceanic crust overlain by the Cretaceous-Palaeocene sedimentary cover (Decandia and Elter, 1969; Marroni et al., 2001; Pandeli et al., 2005); (b) the Subligurian (Eocene-Oligocene) and Tuscan Units, made of evaporite, carbonate and terrigenous, non-metamorphic to very low-grade metamorphic successions (Kalin et al., 1979), and metamorphic units (blueschist and greenschist facies - Jolivet et al., 1998; Rossetti et al., 1999, 2002; Brogi and Giorgetti, 2012; Bianco et al., 2015) ranging from Palaeozoic to Early Miocene; (c) the Umbria-Marche and Sabina Units, principally consisting of an evaporite succession overlain by platform and pelagic carbonates deposited on the thinning and subsiding Adria continental crust formed from the Triassic to the early Tertiary (Barchi et al., 2010; Cosentino et al., 2010).

The Neogene-Quaternary tectonic evolution of the inner Northern Apennines was characterized by the development of simultaneous, co-axial, and eastward migrating compression (in the outer zone) and extension (in the inner zone) (Elter et al., 1975; Ricci Lucchi, 1986; Ori et al., 1986; Boccaletti et al., 1990; Patacca et al., 1992; Barchi, 2010), with a maximum extension oriented almost parallel to the direction of maximum shortening.

Extension and crustal thinning began in the western side of the Northern Apennines (northern Tyrrhenian sea) since Early-Middle Miocene (Bartole, 1995; Carmignani et al., 1995; Brogi and

Liotta, 2008; Barchi, 2010; Brogi, 2011), while, toward the East, accretion was still active at the front of the orogenic wedge (Malinverno and Ryan 1986; Doglioni, 1991; Gueguen et al., 1997). Today, the accretion of the Apennine orogen is still active in the outer zone of the belt, while in the western sector the compressive structures are partly disrupted by extensional tectonics (Lavecchia, 1988; Barchi, 2010). These extensional processes, characterized by a system of NW–striking normal faults and NE–striking transfer faults, produced numerous Neogene-Quaternary basins filled by marine to continental sediments (Martini and Sagri, 1993; Bartole, 1995; Liotta et al., 1998; Brogi and Liotta, 2008; Mancini et al., 2014; Milli et al., 2017).

Such a Neogene-Quaternary tectonic evolution was accompanied by widespread magmatism in the inner Northern Apennines (Serri et al., 1993; Peccerillo, 2003, 2005; Dini et al., 2005; Acocella and Funiciello, 2006). At present the area is characterized by (i) thinned lithosphere (Calcagnile and Panza, 1981; Locardi and Nicolich, 2005), (ii) a positive regional Bouguer anomaly (Giese et al., 1981), (iii) high heat flow (Della Vedova et al., 2001; Chiodini et al., 2013), (iv) localised and regional uplift (Dallmeyer and Liotta, 1998) and geothermal fluids circulation, in the past (Liotta et al., 2010; Zucchi et al., 2017) and today (Barbier, 2002; Batini et al., 2003; Bellani et al., 2004; Chiodini et al., 2007).

Furthermore, the area is characterized by widespread travertine deposits (Capezzuoli et al., 2009) that have long been considered as powerful tools for investigating neotectonics and reconstructing palaeoseismic events (Brogi et al., 2017; 2018).

The recent travertine deposits are clear indicators of active tectonics (Brogi and Capezzuoli, 2009; Brogi et al., 2012) and are generally associated to hydrothermal activity and deep carbon dioxide degassing (Barnes et al., 1978; Chiodini et al., 2000), resulting at the surface in numerous tectonically controlled thermal springs (Brogi and Capezzuoli, 2009; Brogi et al., 2012) and CO_2 degassing areas (Chiodini et al., 2004; Minissale, 2004, Frondini et al., 2008). Hydrothermal circulation is favoured by the damaging fluid-flow enhancement related to the fault–fault intersection, well documented for the Tyrrhenian margin of the Central Apennines until the latest Quaternary (Brogi et al., 2010 and references therein).

3. Study areas

The travertine deposits considered in this work (Rapolano Terme, Canino and Tivoli) are key examples of Quaternary travertine bodies for this area. They are strictly related to tectonic activity, circulation of CO_2 enriched hydrothermal fluids and are characterized by different lithofacies. According to Capezzuoli et al. (2014), travertine is a continental calcium carbonate deposit related to the circulation of non-marine hydrothermal waters. The different lithofacies typically make up travertines (Pentecost, 2005), can be divided in (i) abiotically, related to physical and chemical processes controlled by high temperature, turbulence and water composition, and (ii) biotically, instead related to biological processes as well as to CO_2-degassing and water cooling creating more favourable life conditions (Pentecost, 1990; Jones and Renaut, 1995; Guo and Riding, 1994; Rainey and Jones, 2009; Fouke, 2011; Gandin & Capezzuoli 2014; Della Porta, 2015). The Rapolano Terme travertines mainly formed in a slope environment where crystalline facies (related to abiotic processes) are dominant and porosity is consequently low-medium. On the contrary, Canino and Tivoli travertine systems are dominantly characterized by biotically-related (microbial) lithofacies typical of distal environments and generally characterized by medium-high porosity.

3.1 Rapolano Terme travertines

Rapolano Terme (Fig. 2a) is located in the eastern side of the Siena-Radicofani Basin (Bossio et al., 1993; Brogi, 2011), a 90 Km long, NNW-SSE structural depression developed during Neogene extension and filled by Early-Middle Pliocene marine and Quaternary continental deposits made of gravel, sand, clay and travertine deposits (Bertini et al., 1991; Carmignani et al., 1994; Liotta et al., 1998; Costantini et al., 2009). The Pleistocene-Holocene travertine deposits cover an area of about 14 km^2 with an average thickness of 50 m, and deposited by hydrothermal fluids discharged by thermal springs (Brogi and Capezzuoli, 2009). Depositional environment results mainly formed by several, coalescent slope systems (Brogi et al., 2010) laterally passing to palustrine and fluvio-lacustrine ones (Cipriani et al., 1972; Guo and Riding 1992, 1994, 1998, 1999; Guo et al. 1996; Brogi and Capezzuoli 2009). Presently, the travertine deposits are intensely quarried for ornamental stone.

Both the travertine and the active thermal springs are aligned along the Rapolano fault (Carrara et al., 1998; Minissale et al., 2002), a regional normal fault, NNW-SSE striking (Costantini et al., 2009), which bounds the eastern margin of the Siena-Radicofani Basin and separates the Neogene sediments from the pre-Neogene units exposed in the Rapolano-Trequanda Ridge (pre-Neogene marine carbonate and turbidite succession of the non-metamorphic Tuscan Succession – Losacco, 1952; Bernoulli et al., 1979; Kalin et al., 1979; Decandia et al., 1993; Lazzarotto et al., 2003).

Today the thermal springs are characterised by temperatures up to 38°C, high salinity, $Ca\text{-}SO_4$ composition and a total discharge rate of about 40 l/s (Celati et al., 1990; Frondini 2008; Frondini et al., 2008). The recharge zone of the thermal aquifer roughly coincides with the Mesozoic carbonate rocks exposed in the Rapolano-Trequanda Ridge (Brogi et al., 2007), even if its area is not well defined. The recharge area of the geothermal system can be estimated in 5.7±2.5 km^2; the average flow rate per unit area of similar spring systems is considered to be 7±3 l/km^2 (Celati et al., 1990).

3.2 Canino travertines

Canino area (Fig. 2b) is located 80 km north-west of Rome and is characterized by a broad plain, of about 80 km^2, mostly covered by travertine (about 70 km^2) whit a thickness ranging from a few to more than 100 m (Carrara, 1994). Travertines overlie the Miocene-Pliocene sediments and the

Quaternary pyroclastics and lava flows, this latter related to the alkali potassic volcanism of the Vulsini Mts (Peccerillo, 2005). The plain is limited, (i) to the west by the Fiora River and by the Romani Mts ridge, where crop out the phyllite and quartzites of the Palaeozoic and Triassic metamorphic basement (Dessau et al., 1972), and (ii) to the north-east by the structure of Canino Mt. composed by non-metamorphic Mesozoic carbonates and terrigenous successions of the Tuscan Units (Cocozza, 1963).

The deposition of travertines, started in Middle Pleistocene and is still active, is connected to an intense hydrothermal activity (Carrara, 1994) and figured out by several thermal springs discharging Ca-SO_4 and Na-Cl waters (up to 200 l/s; Chiodini et al., 1991) with high salinity, high pCO_2 and temperatures up to 50°C. The resulting depositional system is mainly composed by depressional environments (Guo and Riding, 1998) representing the extensive, distal portion of the eastern-located thermal springs. The shallower aquifer is almost completely hosted within the travertine deposit and is partly recharged by the carbonate units exposed in the Canino Mt. The aquifer release CO_2 to the atmosphere when groundwater is discharged at the surface from springs. Here, a large part of the discharged groundwater is drained by small streams where water rapidly degasses and total carbon and carbonic acid contents decrease of about one order of magnitude in the first hundred meters: as a consequence, the waters become strongly oversaturated with respect to calcite and precipitate travertine (Chiodini et al., 1999).

3.3 Tivoli travertines

The Acque Albule Basin (Faccenna et al., 2008; Fig. 2c) is located west of Tivoli village (Latium, Central Italy), about 30 Km east of Rome. The basin is confined by the Neogene Appenine fold and thrust belt to the north and to the east (i.e. Cornicolani-Lucretili and Tiburtini Mts.), by the Pleistocene quiescent volcano complex of Colli Albani to the south (Karner et al., 2001) and to the west by the Tiber valley, formed during the Pliocene-Quaternary period (De Filippis et al., 2013) and related with the Tyrrhenian extensional domain. According to De Filippis et al. (2013), the Acque Albule Basin could be considered as a pull-apart basin: faults, mostly NW-striking and extensional (Alfonsi et al., 1991), was accompanied by transverse or oblique (N-NE-striking) strike-slip faults, acting as accommodation structures between the different extensional sectors. The basin is worldwide famous for the *Lapis Tiburtinus* (stone of Tivoli) travertine deposits, used to create many monuments by the early Roman architects. The *Lapis Tiburtinus* travertine, covering an area of more than 20 Km^2, is overlaying the local Plio-Pleistocene alluvial, lacustrine, and epivolcanic deposits, and the Meso-Cenozoic marine carbonate succession (La Vigna et al., 2013). Travertine deposition developed mostly in an over logged, flat environment (Erthal et al., 2017) occurring after or concurrently with the last volcanic phase activity of the Region, during the Late Pleistocene (Faccenna et al., 2008). The *Lapis Tiburtinus* reaches a maximum thickness of 90 m along a N-S line crossing the Acque Albule Basin, with an average thickness of 60 m. The local thermal (23-24° C; La Vigna et al., 2013), $Ca\text{-}SO_4$ rich waters, are enriched by large quantity of CO_2 derived mainly by the decarbonation of Meso–Cenozoic limestones and mantle degassing (Chiodini et al., 2001; Minissale et al., 2002), with recharge area to the north, northeast and east of the basin (Lucretili-Tiburtini and Cornicolani Mts.; La Vigna et al., 2013; Carucci et al., 2012). The most important hydrothermal springs, characterised by T ~23 °C, pH 6.0-6.2 and associated CO_2, and H_2S emissions (Pentecost and Tortora 1989; Minissale et al., 2002; Minissale, 2004; Carucci et al., 2012; La Vigna et al., 2013; Di Salvo et al., 2013) are located in the central part of the plain (Regina Lake; ~1850 l/s and Colonnelle Lake; ~250 l/s; La Vigna et al., 2013). The total natural discharge of the system is about 4000 l/s corresponding to a recharge area of about 220 Km^2 (Boni et al., 1986; Chiodini et al., 2000).

4. Methods

For the estimation of the CO_2 flux released to the atmosphere during travertine deposition it is necessary to know the age of the travertines, their volume and their average $CaCO_3$ content.

The absolute ages and the periods of travertine formation are quite well known for the three study areas (Taddeucci and Voltaggio, 1987; Carrara, 1994; Minissale et al., 2002; Minissale, 2004). The volumes of the travertine deposits have been estimated using a 3D geological model, developed for each study area, based on available data refined by some new field observations.

Finally, for evaluating the average $CaCO_3$ content, 86 travertine samples have been collected and analyzed (29 at Rapolano; 34 at Canino; 23 at Tivoli).

4.1 Age of the travertine deposits

For the ages of the three travertine deposits, which all developed during the Pleistocene, we refer to the values obtained by uranium-series disequilibrium datings reported in literature:

- at Rapolano travertine deposition started at 157 ± 15 Ka in the southern part of the deposit (Brogi et al., 2010) and is still active today in its northern part (Guo and Riding, 1992, 1994, 1998, 1999);
- at Canino the lowermost part of the succession was dated by Radtke et al. (1976) at 300 Ka and by Carrara et al. (1994) at more than 350 Ka. No travertines with ages between 300 Ka and 237 Ka are present and most deposits are younger than 200 Ka (Taddeucci and Voltaggio, 1987; Carrara et al., 1994). The base of the succession, excluding the oldest travertine that are almost completely eroded, is dated between 237 and 181 Ka (209 ± 28 Ka on average - Carrara et al., 1994);
- the beginning of travertine deposition in the Acque Albule Basin (Tivoli) started at 115 ± 8 Ka and, according to Faccenna et al. (2008), continued till 28 ± 16 Ka, covering an interval of deposition of 87 ± 24 Ka. At present deposition occurs only in some very minor seeps forming very limited amounts of travertine, At present deposition occurs only in some very

minor seeps forming very limited amounts of travertine, even if degassing is still active in a large part of the Tivoli area.

4.2 Estimation of the travertine deposits volumes

Digital Elevation Models (DEM) have been computed for each study area, using elevation data from aerial photos, topographic maps and new GPS data collected during field work. Areas of travertine outcrops were delineated (Fig. 2) based on the available geological maps (Chiodini et al., 1991; Faccenna et al., 2008; Brogi and Capezzuoli, 2009). Finally, new detailed field observations (supplementary material 1), integrated with the available stratigraphic data (Chiodini et al., 1991; Carrara, 1994; Faccenna et al., 2008; Brogi and Capezzuoli, 2009) allowed to reconstruct the thicknesses of travertine successions and to interpolate isopach lines for each deposit (Fig. 3). The shape of the deposits and their volumes were estimated intersecting the DEM surfaces with surfaces representing the base of the travertines (Fig. 3).

4.3 Determination of the carbonate content and porosity of the travertine samples

In order to determine $CaCO_3$ content and porosity of the travertines, a portion of each sample has been dried and weighted with a high precision balance (precision 0.001 g) and its bulk volume has been determined by water displacement after coating the rock surface with paraffin. Then its bulk density has been computed from the weight/volume ratio and the sample porosity has been inferred from

$$p = 1 - (\rho_b/\rho_p) \qquad (2)$$

where ρ_b is the bulk density and ρ_p is the particle density (assumed to be 2.7 g cm^{-3}, being the density of calcite).

For the determination of the $CaCO_3$ fraction a known amount (some grams) of each sample has been dissolved in a 5M HCl solution. Each solution has been filtered with a cellulose acetate 0.45 µm membrane filters and the insoluble residue has been dried and weighted. The carbonate fraction of each travertine sample has been computed from:

$$f\,CaCO_3 = (W_i - W_r)/W_i \qquad (3)$$

where W_i is the initial weight and W_r the weight of the insoluble fraction.

4.4 Determination of the CO_2 flux associated to travertine deposition

The total moles of $CaCO_3$ of each travertine deposit have been computed from

$$\text{moles } CaCO_3 = (V \times \rho_b \times f\,CaCO_3)/M \qquad (4)$$

where V is the volume of the deposit, ρ_b is the average bulk density of the travertine, $f\,CaCO_3$ is the fraction of $CaCO_3$ in the travertine and M is the molar mass of $CaCO_3$. According to equation (1), the moles of $CaCO_3$ correspond to the cumulative amount of CO_2 degassed during travertine deposition.

Finally, the CO_2 discharge rate (F-CO_2) has been computed dividing the moles of $CaCO_3$ by the duration of the travertine formation and the average CO_2 flux (f-CO_2) has been computed dividing F-CO_2 by the area of the hydrological basin feeding the travertine-depositing CO_2-rich springs.

5. Results

The three study areas are characterised by different surface extensions of the travertine outcrops: i.e. Rapolano, 3.9 Km^2; Canino, 70 Km^2; Tivoli, 26 Km^2. The volumes of the deposits, as calculated through the 3D geological models, are: 0.046 km^3 for Rapolano; 0.9 km^3 for Canino; 1.1 km^3 for Tivoli (Fig. 3).

The central tendency, the tendency of quantitative data to cluster around some central value, and the variability of porosity and $CaCO_3$ fraction (reported as weight %) are summarized in Table 1 (full dataset in supplementary material 2). Porosity values range from 0.27% to 30.68% and show a positively skewed distribution (Fig. 4a) with a mean (12.14%) being greater than the median (10.68%). Rapolano and Tivoli samples show similar porosity values (median values of 8.45% and 9.05%, respectively) while Canino samples are characterized by a higher porosity (median = 16.78%).

The $CaCO_3$ content is very similar in the three areas (median values of 98.34%, 99.09% and 99.29% respectively). Considering the whole dataset, the distribution is characterized by a left skewed log-normal distribution (Fig. 4b) with a median (99.09%) higher than arithmetic mean (97.44%) and a very small variability (interquartile range, IQR = 2.89%).

Considering that both porosity and $CaCO_3$ content do not follow a gaussian distribution, the median values are more representative of the central tendency with respect to the arithmetic mean and have been used in calculations of F-CO_2 and $f$$CO_2$.

The results of the CO_2 flux calculations are summarized in Table 2.

In the three areas considered in the present work, the CO_2 discharge rates estimated through the volume of the travertine deposits (F-CO_2) range from $(1.11 \pm 0.02) \times 10^6$ mol y^{-1} at Rapolano to $(26.49 \pm 0.69) \times 10^6$ mol y^{-1} at Tivoli. Despite the large differences in F-CO_2 values, the resulting f-

F-CO_2 values, that is the specific CO_2 discharge per unit area, are rather uniform, ranging in a very small interval between (1.24 ± 0.12) $\times 10^6$ mol y^{-1} km^{-2} and (1.38 ± 0.42) $\times 10^6$ mol y^{-1} km^{-2} (Tab. 2).

6. Discussion

In western central Italy, travertines are mostly associated to spring systems discharging to the surface warm, CO_2 rich and acidic waters. Groundwaters circulate into carbonate aquifers hosted by Jurassic-Cretaceous formations, where they increase their pCO_2 and dissolve carbonate minerals (Frondini, 2008). The high CO_2 content of groundwater is principally caused by the high flux of endogenous CO_2 characterizing the region (Chiodini et al., 2000, 2004) as confirmed by the isotopic analysis of both dissolved inorganic carbon of groundwater (Chiodini et al., 2000, 2004) and calcite in travertines (Panichi and Tongiorgi, 1975; Manfra, 1976; Minissale et al., 2002). When groundwaters are discharged by springs they re-equilibrate to the surface conditions degassing CO_2 and rapidly precipitating solid carbonates. Through this process the amount of deposited travertine is directly linked to the amount of CO_2 degassing from the groundwater, which is proportional to the influx of deep CO_2 into the aquifers. In this kind of systems, the estimation of the volumes and $CaCO_3$ fraction of travertines (of known age) is a proxy to estimate the average CO_2 discharged by the system since the beginning of travertine deposition.

In the diagram F-CO_2 values vs recharge area (Fig. 5), the three study areas are compared to the geothermal systems and spring systems of the region. Our data roughly plot along the same line, just above the global baseline of CO_2 fluxes from high heat flow regions (10^6 mol y^{-1} km^{-2} - Kerrick et al., 1995), suggesting that, at least in the western Apennine region, the degassing processes are characterized by scale invariance: the CO_2 flux (*f*-CO_2) doesn't change significantly when scales (F-CO_2 and recharge area) are multiplied by a common factor.

The deduced CO_2 fluxes associated to travertine deposition (i) fall in the range of the present day deep CO_2 fluxes of western central Italy (10^5 to 10^7 mol y^{-1} km^{-2} - Chiodini et al., 2000), (ii) are slightly higher than the global baseline of CO_2 fluxes from high heat flow regions (10^6 mol y^{-1} km^{-2} - Kerrick et al., 1995), (iii) are lower but of the same order of magnitude of the current CO_2 flux of medium-high enthalpy geothermal systems in central Italy, ranging from 2×10^6 to 8×10^6 mol y^{-1} km^{-2} (Gambardella et al., 2004).

The estimated *f*-CO_2 values, that represent the time averaged CO_2 fluxes of each study area, are a minimum estimation of the deep CO_2 degassing processes, because part of the travertine deposits may have been eroded. As reported in Parise et al. (2008) dissolution and erosion affect the carbonate rocks, especially travertines in different ways. Such processes are influenced by latitude, temperature, and biological activity and strongly depend on the climatic zone.

A further cause of underestimation of the CO_2 flux is the possible CO_2 loss from the thermal water before travertine deposition starts. Often CO_2-charged thermal waters are undersaturated with respect to carbonate minerals and reach oversaturation only after loosing part of the dissolved CO_2. This part does not create recognizable deposits. In some cases deep groundwaters are characterised by very high pCO_2 (>1 bar) and can lose a significant part of their CO_2 content from bubbling pools or dry gas emissions (e.g. Rogie et al., 2000; Gulec et al., 2002; Mutlu et al., 2008).

The extent of the underestimation can be roughly evaluated by comparing the results of our calculations to the direct measurements of CO_2 flux or to the carbon mass and isotopic balance of the acquifers feeding the springs, when available (Chiodini et al., 1999; Chiodini et al., 2000).

At Rapolano the possible underestimation is not valuable but can be significant only in the southern part of the study area, where bubbling pools and CO_2 vents are present. At Canino our estimation is about 70% of the value computed from the carbon mass balance (see Fig.6). At Tivoli, travertine deposition is very limited nowadays, but CO_2 degassing is still very strong: the average specific flux computed with the methods proposed in this work is about 66% of the present day specific CO_2

flux computed from the carbon balance of the Prenestini Mts aquifer (the aquifer feeding Tivoli springs) by Chiodini et al. 2000 ($1.86x10^6$ vs $2.78x10^6$ mol/km^{-2} y^{-1}).

Our data, although they are a minimum estimate of the CO_2 degassing process, are in agreement with earlier studies (Chiodini et al., 2000, 2004; Frondini et al., 2008) and confirm that western central Italy is a globally relevant source of (deeply mantle derived and metamorphic) carbon.

The CO_2 degassing process that is currently affecting the region was active, with similar discharge rates, at least since 200 Ka ago (probably more, considering that the older, eroded travertines at Canino were dated by Carrara et al. (1994) at more than 350 Ka). Other travertine deposits in western central Italy, for which $^{234}U/^{230}Th$ and ^{14}C data are available (Fig. 6), fall in the same time interval (e.g. from 268 ± 22 ka to the present at Sarteano - Brogi et al. 2012; 134.8 ± 1.6 Ka at Civita Castellana - Minissale et al., 2002; from 350 to 40 Ka in the Albegna Basin - Vignaroli et al., 2016; 23.216 ± 0.124 Ka Acqua Borra - Brogi et al., 2014; 182 ± 82 Ka San Casciano dei Bagni - Vignaroli et al., 2013) but could be even older, considering that travertine is prone to erosion. The widespread presence of travertine bodies in the study area highlights the temporal continuity of the degassing process in western central Italy from (at least) 350 Ka to the present.

6. Conclusion

A better quantification of diffuse degassing is necessary to constrain the global carbon cycle and to give a realistic estimate of the CO_2 degassing process at a global scale (Frondini et al., 2018).

The proposed method is an independent approach to estimate CO_2 fluxes related to direct measurements; the similarity of the results obtained by the two methods supports the reliability of its outcome and suggests the possibility of its applications to other areas characterized by travertine deposits.

Considering the widespread occurrence of travertine deposits in geothermal areas, active fault zones, volcanic and seismic regions, the proposed approach can be used as a tool to compute the deep CO_2 flux in several tectonically active areas of the world.

In particular, computing the CO_2 fluxes from the volumes and the ages of travertine deposits may be useful in order (i) to compare the present-day CO_2 fluxes to the time integrated paleo CO_2 fluxes, (ii) to estimate a baseline CO_2 flux in large regions where direct measurements are not easily achievable and (iii) to study the Earth degassing process in seismically active fault zones.

Acknowledgements

We wish to thank Tonguç Uysal and an anonymous reviewer for their useful comments and constructive criticisms that substantially improved our manuscript. This work was partly financially supported by Department of Physics and Geology, University of Perugia and University of KU Leuven.

References

Acocella, V., Funiciello, R., 2006. Transverse systems along the extensional Tyrrhenian margin of central Italy and their influence on volcanism. Tectonics, 25.

Alfonsi, L., Funiciello, R., Mattei, M., 1991. Strike-slip tectonics in the Sabina area", Bollettino della Società Geologica Italiana, 110, 481-488.

Altunel, E., 2005. Travertines: neotectonic indicators. In: Travertine, Proceedings of 1st International Symposium on Travertine (Eds M. Ozkul, S. Yagiz and B. Jones), pp. 105-106. September 21–25, 2005, Denizli, Turkey. Kozan Offset, Ankara.

Altunel, E., Hancock, P.L., 1993a. Active fissuring and faulting in Quaternary travertines at Pamukkale, Western Turkey. Zeitschrift für Geomorphologie Supplement, 94, 285–302.

Altunel, E., Hancock, P.L., 1993b. Morphology and structural setting of Quaternary travertines at Pamukkale, Turkey. Geol. J., 28, 335–346.

Banerjee, A., Person, M., Hofstra, A., Sweetkind, D., Cohen, D., Sabin, A., Unruh, J., Zyvoloski, G., Gable, C.W., Crossey, L. and Karlstrom, K., 2011. Deep permeable fault-controlled helium transport and limited mantle flux in two extensional geothermal systems in the Great Basin, United States. Geology, 39, 195–198.

Barbier, E., 2002, Geothermal energy and current status: an overwiew. Renew. Sust. En. Rev. 6, 3-65.

Barchi, M., 2010. The Neogene-Quaternary evolution of the Northern Apennines: crustal structure, style of deformation and seismicity. In: (Beltrando, M., Peccerillo, A., Mattei, M., Conticelli, S., and Doglioni, C. Eds) The Geology of Italy: tectonics and life along plate margins, Journal of the Virtual Explorer, Electronic Edition, ISSN 1441-8142, volume 36, paper 11, doi:10.3809/jvirtex.2010.00220

Barnes, I., Irwin, W., White, D., 1978. Global distribution of CO_2 and major zones of seismicity. U.S. Geol. Surv., Open-File Rep.78-39.

Bartole, R., 1995. The North Tyrrhenian–Northern Apennines post-collisional system: constraints for a geodynamic model. Terra Nova 7, 7-30.

Batini, F., Brogi A., Lazzarotto A., Liotta D., Pandeli E., 2003. Geological Features of Larderello-Travale and Mt. Amiata Geothermal Areas (Southern Tuscany, Italy). Episodes 26, 239-244

Bellani, S., Brogi, A., Lazzarotto, A., Liotta, D., Ranalli, G., 2004. Heat flow, deep temperatures and extensional structures in the Larderello Geothermal Field (Italy): Constraints on geothermal fluid flow. J. Volcanol. Geotherm. Res. 132, 15-29.

Berner, R.A., 1993. Weathering and its effect on atmospheric CO_2 over Phanerozoic time. Chem. Geol. 107, 373-374.

Berner, R.A., 2004. The Phanerozoic Carbon Cycle: CO_2 and O_2. Oxford University Press, p. 158.

Berner, R.A., 2006. GEOCARBSULF: A combined model for Phanerozoic atmospheric O_2 and CO_2. Geochim. Cosmochim. Acta 70, 5653-5664.

Berner R.A., Lasaga, A.C., Garrels, R.M., 1983. The carbonate-silicate geochemical cycle and its effect on atmospheric carbon dioxide over the past 100 million years. Am. J. Sci. 283, 641-683.

Bernoulli, D., Kàlin, O., Pattaca, E., 1979. A sunken continental margin of the Mesozoic Tethys: the Northern and Central Apennines. Assoc. Sedimentol. Fr. Publ. Spec, 1, 197-210.

Bertini, G., Cameli, G.M., Costantini, A., Decandia, F.A., Di Filippo, M., Dini, I., Elter, F.M., Lazzarotto, A., Liotta, D., Pandeli, E., Sandrelli, F., Toro, B., 1991. Struttura geologica fra i monti di Campiglia e Rapolano Terme (Toscana meridionale): stato attuale delle conoscenze e problematiche, Studi Geologici Camerti, Vol. spec. 1991/1 155-178.

Bianco, C., Brogi, A., Caggianelli, A., Giorgetti, G., Liotta, D., Meccheri, M., 2015. HP-LT metamorphism in Elba Island: implications for the geodynamic evolution of the inner Northern Apennines (Italy). J. Geodyn. 91, 13–25.

Boccaletti, M., Calamita, F., Deiana, G., Celati, R., Massari, F., Moratti, G., Ricci Lucchi, F., 1990. Migrating foredeep-thrust belt systems in the northern Apennines and southern Alps. Palaeogeography, Palaeoclimatology, Palaeoecology, 77, 3-14.

Boni, C.F., Bono, P., Capelli, G., 1986. Schema Idrogeologico dell'Italia Centrale. Mem. Soc. Geol. It., 35, 991-1012.

Bosence, D., Gibbons, K., Le Heron, D.P., Morgan W.A., Pritchard, T., Vining, B.A., 2015. Microbial carbonates in space and time: introduction. Special Publications, Geological Society of London, 418, 1-15.

Bossio, A., Costantini, A., Lazzarotto, A., Liotta, D., Mazzanti, R., Mazzei, R., Salvatorini, G.F., Sandrelli, F., 1993. Rassegna delle conoscenze sulla stratigrafia del Neoautoctono toscano, Mem. Soc. Geol. It., 49, 17–98.

Brancaccio, L., D'Argenio, B., Ferreri, V., Stanzione, D., Taddeucci, A., Voltaggio, M., 1988. I travertini di Rocchetta al Volturno (Molise): datazioni con 230Th e modello deposizionale. Mem. Soc. Geol. It., 41, 673-683.

Brogi, A., Capezzuoli, E., Gandin, A., 2007. I travertini delle Terme di S.Giovanni (Rapolano Terme, appennino settentrionale) e loro implicazione neotettonica. Il Quaternario (Italian Journal of

Quaternary Sciences), 20(2), 107-124.

Brogi A., Liotta D., 2008. Highly extended terrains, lateral segmentation of the substratum and basin development: the Middle-Late Miocene Radicondoli Basin (Inner Northern Apennines, Italy), Tectonics, 27, 1-20.

Brogi, A., Capezzuoli, E., 2009. Travertine deposition and faulting: the fault-related travertine fissure-ridge at Terme S. Giovanni, Rapolano Terme (Italy). International Journal of Earth Sciences, 98, 931–947.

Brogi, A., Capezzuoli, E., Aqué, R., Branca, M., Voltaggio, M., 2010. Studying travertine for neotectonics investigations: Middle–Late Pleistocene syn- tectonic travertine deposition at Serre di Rapolano (Northern Apennines, Italy). Geologische Rundschau, 99, 1383–1398.

Brogi, A., 2011. Bowl-shaped basin related to low-angle detachment during continental extension: The case of the controversial Neogene Siena Basin (central Italy, Northern Apennines). Tectonophysics, 499, 54-76

Brogi, A., Capezzuoli, E., Buracchi, E., Branca, M., 2012. Tectonic control on travertine and calcareous tufa deposition in a low-temperature geothermal system (Sarteano, Central Italy). J. Geol. Soc., London 169, 461-476.

Brogi, A., Giorgetti, G., 2012. Tectono-metamorphic evolution of the siliciclastic units in the Middle Tuscan Range (inner Northern Apennines): Mg-carpholite bearing quartz veins related to syn-metamorphic syn-orogenic foliation. Tectonophysics, 526-529, 167-184.

Brogi, A., Capezzuoli, E. 2014. Earthquake impact on fissure-ridge type travertine deposition. Geological Magazine, 151, 1135–1143.

Brogi, A., Capezzuoli, E., Martini, I., Picozzi, M., Sandrelli, F., 2014. Late Quaternary tectonics in the inner Northern Apennines (Siena Basin, southern Tuscany, Italy) and their seismotectonic implication. Journal of Geodynamics, 76, 25–45.

Brogi A., Liotta D., Ruggieri G., Capezzuoli E., Meccheri M., Dini A., 2016. An overview on the characteristics of geothermal carbonate reservoirs in southern Tuscany. Ital. J. Geosci. 135, 17-29.

Brogi, A., Capezzuoli, E., Kele, S., Baykara, M.O., Chuan-Chou, S., 2017. Key travertine tectofacies for neotectonics and palaeoseismicity reconstruction: effects of hydrothermal overpressured fluid injection. Journal of the Geological Society, 174, 4.

Brogi, A., Capezzuoli, E., Moretti, M., Olvera-García, E., Matera, P.F., Garduno-Monroy, V-H., Mancini, A., 2018. Earthquake-triggered soft-sediment deformation structures (seismites) in travertine deposits. Tectonophysics, 745, 349-365.

Burton, M.R., Sawyer G.M., Granieri, D., 2013. Deep Carbon Emissions from Volcanoes. Rev. Min. Geochem. 75, 323-354. D

Calcagnile, G., Panza, G.F., 1981. The main characteristics of the lithosphere-asthenosphere system in Italy and surrounding regions. Pure Appl. Geophys., 119, 865-879.

Calderoni, G., Cilla, G., Dramis, F., Esu, D., Magnatti, M., Materazzi, M., 1996. La deposizione di tarvertino nelle aree prossimali dei Fiumi Esino, Potenza e Chienti durante l'Olocene antico (Appennino centrale marchigiano). Il Quaternario, 9(2), 481-492.

Capezzuoli, E., Gandin, A., Pedley, H.M., 2009. Travertines and calcareous tufa in Tuscany (Central Italy). 27th IAS Meeting of Sedimentology, Alghero, Italy. Fieldtrip Guidebook, v.129, pp. 158.

Capezzuoli, E., Gandin, A., Sandrelli, F., 2010. Calcareous tufa as indicators of climatic variability: a case study from southern Tuscany (Italy). Geological Society, London, Special Publications, 336, 263-281. https://doi.org/10.1144/SP336.14

Capezzuoli, E., Gandin, A., Pedley, M., 2014. Decoding tufa and travertine (fresh water carbonates) in the sedimentary record: The state of the art. Sedimentology, 61, 1-21.

Cardellini, C., Chiodini, G., Frondini, F., Avino, R., Bagnato, E., Caliro, S., Lelli, M., Rosiello, A., 2017. Monitoring diffuse volcanic degassing during volcanic unrests: the case of Campi Flegrei (Italy). Scientific Reports, 7, 6757, https://doi.org/10.1038/s41598-017-06941-2

Carmignani, L., Decandia, F.A., Fantozzi, P.L., Lazzarotto, A., Liotta, D., Meccheri, M., 1994. Tertiary Extensional Tectonics in Tuscany (Northern Apennines, Italy). Tectonophysics, 238, 295-315.

Carmignani, L., Decandia, F.A., Disperati, L., Fantozzi, P.L., Lazzarotto, A., Liotta, D., Oggiano, G., 1995. Relationships between the Sardinia-Corsica-Provençal Domain and the Northern Apennines. Terranova 7, 128–137.

Carminati, E., Doglioni, C., 2012. Alps vs. Apennines: the paradigm of a tectonically asymmetric Earth. Earth-Sci. Rev., 112, 67-96.

Carrara. C., 1994. I travertini di Canino (Viterbo, Italia Centrale): Elementi di Cronolitostratigrfia, di Geochimica Isotopica e loro significato ambientale e climatico. Il Quaternario 7, 73–90.

Carrara, C., Ciuffarella, L., Paganin, G., 1998. Inquadramento geomorfologico e climatico - ambientale dei travertini di Rapolano Terme (SI). Il Quaternario, 11, 319-329.

Carrara, C., 1998. I tarvertini della Valle del Pescara tra Popoli e Tor de' Passeri (Abruzzo, Italia Centrale). Il Quaternario, 11(2), 163-178.

Carrara, C., Branca, M., Pisegna, E., Verrubbi, V., Voltaggio, M., 2006. Calcareous tufa deposits of the Aniene Valley between Vallepietra and Mandela-Vicovaro (Latium, Central Italy). Il Quaternario, 19(1), 19-44.

Carucci, V., Petitta, M., Aravena, R., 2012. Interaction between shallow and deep aquifers in the Tivoli Plain (Central Italy) enhanced by groundwater extraction: A multi isotope approach and geochemical modeling. Appl. Geochem., 27, 266-280.

Celati, R., Grassi, S., Calore. C., 1990. Overflow thermal springs of Tuscany (Italy). J. Hydrol., 118,191 - 207.

Chafetz, H.S., Folk, R.L., 1984. Travertines: depositional morphology and the bacterially constructed constituents. J. Sedim. Petrol., 54, 289–316.

Chiodini, G., Giaquinto, S., Frondini, F., Santucci, A., 1991. Hydrogeochemestry and hydrogeology of the Canino hydrothermal system (Italy). Geothermics, 20-5/6, 329-342.

Chiodini, G., Frondini, F., Kerrick, D.M., Rogie, J., Parello, F., Peruzzi, L., Zanzari, A.R., 1999. Quantification of deep CO_2 fluxes from Central Italy. Examples of carbon balance for regional aquifers and of soil diffuse degassing. Chem. Geol 159, 205-222.

Chiodini, G., Frondini, F., Cardellini C., Parello F., Peruzzi, L., 2000. Rate of diffuse carbon dioxide Earth degassing estimated from carbon balance of regional aquifers: The case of central Apennine, Italy, J. Geophys. Res., 105, 8423–8434.

Chiodini, G., Frondini F., 2001. Carbon dioxide degassing from the Albani Hills volcanic region, Central Italy. Chem Geol. 177, 67-83.

Chiodini, G., Cardellini, C., Amato, A., Boschi, E., Caliro. S., Frondini, F., Ventura, G., 2004. Carbon dioxide Earth degassing and seismogenesis in central and southern Italy. Geophys. Res. Lett. 31(7): L07615.

Chiodini, G., Baldini, A., Barberi, B., Carapezza, M.L., Cardellini, C., Frondini, F., Granieri, D., Ranaldi, M., 2007. Carbon dioxide degassing at Latera caldera (Italy): Evidence of geothermal reservoir and evaluation of its potential energy. J Geophys. Res 112, B12204.

Chiodini, G., Cardellini, C., Caliro, S., Chiarabba, C., Frondini, F., 2013. Advective heat transport associated with regional Earth degassing in central Apennine (Italy). Earth Planet. Sci. Lett. 373, 65–74.

Cipriani, N., Ercoli, A., Malesani, P., Vannucci, S., 1972. I travertini di Rapolano Terme (Siena). Mem. Soc. Geol. It., 11, 31-46.

Claes, H., Soete, J., Van Noten, K., El Desouky, H., Erthal, M.M., Vanhaecke, F., Özkul, M., Swennen, R., 2015. Sedimentology, three-dimensional geobody reconstruction and carbon dioxide origin of Pleistocene continental carbonate deposits in the Ballık area (south-west Turkey). Sedimentology, 62, 1408–1445.

Claes, H., Marques-Erthal, M., Soete, J., Özkul, M., Swennen, R., 2017. Shrub and pore type classification: Petrography of travertine shrubs from the Ballık-Belevi area (Denizli, SW Turkey). Quaternary International. 217, 147–163.

Cocozza, T., 1963. Nuovi dati stratigrafici e tettonici sul Monte Canino (Viterbo). Geol. Romana, 1, 15-40.

Cosentino, D., Cipollari, P., Marsili, P., Scrocca, D., 2010. Geology of the central Apennines: a regional review. In: Beltrando, M., Peccerillo, A., Mattei, M., Conticelli, S., Doglioni, C. (Eds) The Geology of Italy: tectonics and life along plate margins, Journal of the Virtual Explorer, Electronic Edition, ISSN 1441-8142, volume 36, paper 12, doi:10.3809/jvirtex.2010.00223

Costantini, A., Decandia, F.A., Lazzarotto, A., Liotta, D., Mazzei, R., Pascucci, V., Salvatorini, G., Sandrelli, F., 2009. Note illustrative della Carta Geologica d’Italia alla scala 1:50.000 foglio 296 SIENA, ISPRA Servizio Geologico d’Italia, 123.

Crossey, L., Karlstrom, K.E., Springer, A.E., Newell, D., Hilton, D.R., Fischer, T., 2009. Degassing of mantle-derived CO_2 and He from springs in the southern Colorado Plateau region-Neotectonic connections and implications for groundwater systems. Geol. Soc. Am. Bull. 121, 1034-1053.

D'Alessandro, W., Giammanco, S., Bellomo, S., Parello, F., 2007. Geochemistry and mineralogy of travertine deposits of the SW flank of Mt. Etna (Italy): Relationships with past volcanic and degassing activity. J. Volcanol. Geotherm. Res., 165, 64-70.

Dallmeyer, R.D., Liotta, D., 1998. Extension, uplift of rocks and cooling ages in thinned crustal provinces: the Larderello geothermal area (inner Northern Apennines, Italy). Geol. Mag., 135, 193-202

Decandia, F.A., Elter, P., 1969. Riflessioni sul problema delle ofioliti nell'Appennino Settentrionale (Nota preliminare). Atti Soc. Tosc. Sc. Nat., Mem., ser. A,76, 1-9.

Decandia, F.A., Lazzarotto, A., Liotta, D., 1993. La Serie ridotta nel quadro dell'evoluzione geologica della Toscana meridionale, Mem Soc Geol I t49, 181–190.

De Filippis, L., Faccenna, C., Billi, A., Anzalone, E., Brilli, M., Soligo, M., Tuccimei, P., 2013. Plateau versus fissure ridge travertines from Quaternary geothermal springs of Italy and Turkey: Interactions and feedbacks between fluid discharge, paleoclimate, and tectonics. Earth-Sci.Rev., 123, 35-52.

Della Porta, G., 2015. Carbonate build-ups in lacustrine, hydrothermal and fluvial settings: Comparing depositional geometry, fabric types and geochemical signature. Geological Society London, Special Publications 418, 1.

Della Porta, G., Croci, A., Marini, M., Kele, S., 2017. Depositional architecture, facies character and geochemical signature of the Tivoli travertines (Pleistocene, Acque Albule Basin, Central Italy). Rivista Italiana di Paleontologia e Stratigrafia (Research In Paleontology and Stratigraphy) 123, 487-540.

Della Vedova, B., Bellani, S., Pellis, G., Squarci, P., 2001. Deep temperatures and surface heat flow distribution. In: Vai G.B. & Martini I.P. (Eds.): "Anatomy of an orogen: the Apennines and adjacent Mediterranean basins". Kluwer Academic Publishers, pp 65-76, Dordrecht, The Netherlands.

Dessau, G., Duchi, G., Steu, B., 1972. Geologia e depositi minerari della zona Monti Romani-Montete (comuni di Manciano e Capalbio, Grosseto) ed Ischia di Castro (Viterbo). Memorie della Societa Geologica Italiana, 11, 217-260.

De Rita, D., Giordano, G., Esposito, A., Fabbri, M., Rodani, S., 2002. Large volume phreatomagmatic ignimbrites from the Colli Albani volcano (Middle Pleistocene, Italy). J. Volc. Geoth. Res., 118, 77-98.

De Rita, D., Faccenna, C., Funiciello, R., Rosa, C., 1995. Structural and geological evolution of the Colli Albani volcanic district. In: Trigila R. (Ed) - The Volcano of the Alban Hills. Rome: Tipografia SGS, 33–71.

Di Salvo, C., Mazza, R., Capelli, G., 2013. Gli acquiferi in travertino del Lazio: schemi idrogeologici e caratteristiche chimico-fisiche. Rend. Online Soc. Geol. It., 27, 54-76.

Dini, A., Gianelli, G., Puxeddu, M., Ruggieri, G., 2005. Origin and evolution of Pliocene–Pleistocene granites from the Larderello geothermal field (Tuscan Magmatic Province, Italy). Lithos 81, 1-31.

Doglioni, C., 1991. A proposal for the kinematic modelling of W-dipping subductions - possible applications to the Tyrrhenian-Apennines system. Terra Nova, 3, 423-434.

Elter P., Giglia G., Tongiorgi M., Trevisan L., 1975. Tensional and compressional areas in the recent (Tortonian to Present) evolution of north Apennines. Bollettino di Geofisica Teorica Applicata 17, 3–18.

Erthal, M.M., Capezzuoli, E., Mancini, A., Claes, H., Soete, J., Swennen, R., 2017. Shrub morpho-types as indicator for the water flow energy – Tivoli travertine case (Central Italy). Sediment. Geol., 347, 79-99.

Faccenna, C., Soligo, M., Billi, A., De Filippis, L., Funiciello, R., Rossetti, C., Tuccimei, P., 2008. Late Pleistocene depositional cycles of the Lapis Tiburtinus travertine (Tivoli, Central Italy): Possible influence of climate and fault activity. Glob. Planet. Change, 63, 299-308.

Fouke, B.W., 2011. Hot-spring Systems Geobiology: abiotic and biotic influences on travertine formation at Mammoth Hot Springs, Yellowstone National Park, USA. Sedimentology, 58, 170, 219.

Ford, T.D., Pedley, H.M., 1996. A review of tufa and travertine deposits of the world. Earth Sci. Rev., 41, 117, 175.

Frondini, F., Chiodini, G., Caliro, S., Cardellini, C., Granieri, D. & Ventura, G. 2004. Diffuse CO_2 degassing at Vesuvio, Italy. Bull. Volcanol., 66, 642–651. DOI:10.1007/s00445-004-0346-x

Frondini, F., 2008. Geochemistry of regional aquifer systems hosted by carbonate-evaporite formations in Umbria and southern Tuscany (central Italy). Appl. Geochem. 23, 2091–2104.

Frondini, F., Caliro, S., Cardellini, C., Chiodini, G., Morgantini, N., Parello, F., 2008. Carbon dioxide degassing from Tuscany and Northern Latium (Italy). Global and Planetary Change, 61, 89-102.

Frondini, F., Cardellini C., Caliro S., Chiodini G., Morgantini N., 2012. Regional groundwater flow and interactions with deep fluids in western Apennine: the case of Narni-Amelia chain (Central Italy). Geofluids (2012) 12, 182–196.

Frondini, F., Cardellini C., Caliro, S., Beddini, G., Rosiello, A., Chiodini, G., 2018. Measuring and interpreting CO_2 fluxes at regional scale: the case of the Apennines, Italy. Journal of the Geological Society (2019) 176, 408–416.

Gaeta, M., Fabrizio, G., Cavarretta G., 2000. F-phlogopites in the Alban Hills Volcanic District (Central Italy): indications regarding the role of volatiles in magmatic crystallisation. J. Volcan. Geoth. Res., 99, 179-193.

Gambardella, B., Cardellini, C., Chiodini, G., Frondini, F., Marini, L., Ottonello, G., Vetuschi, Zuccolini, M., 2004. Fluxes of deep CO_2 in the volcanic areas of central-southern Italy. J. Volcanol. Geotherm. Res. 136, 31.52.

Gandin, A., Capezzuoli, E., 2014. Travertine: distintive depositional fabrics of carbonates from thermal spring systems. Sedimentology, 61, 264-290.

Gerlach, T., 2011. Volcanic versus anthropogenic carbon dioxide. EOS, 92, 201-208.

Giese, P., Wigger, P., Morelli, C., Nicolich, R., 1981. Seismische Studien zur Bestimmung der Krustenstruktur im Bereich der geothermischen Anomalie der Toskana. EUR 7578, de MF, 108 pp.

Google., 2018. Google Earth/Maps; Digital Globe 2018. http://www.earth.google.com

Gueguen, E., Doglioni, C., Fernandez, M., 1997. Lithospheric boudinage in the Western Mediterranean backarc basin. Terra Nova, 9, 184-187.

Güleç, N., Hilton, D. R., Mutlu, H. 2002. Helium isotope variations in Turkey: relationship to tectonics, volcanism and recent seismic activities. Chem. Geol. 187, 129-142.

Guo, L., Andrews, J., Riding, R., Dennis, P., Dresser, D., 1996. Possible microbial effects on stable car- bon isotopes in hot-spring travertines. Jour. Sed. Research, 66, 468-473.

Guo, L., Riding, R., 1992. Micritic aragonite laminae in hot water travertine crusts, Rapolano Terme, Italy. Sedimentology, 39, 37-53.

Guo, L., Riding, R., 1994. Origin and diagenesis of Quaternary travertine shrub fabrics, Rapolano Terme, Central Italy. Sedimentology, 41, 499-520.

Guo, L., Riding, R., 1998. Hot-spring travertine facies and sequences, Late Pleistocene, Rapolano Terme, Italy. Sedimentology, 45, 163-180.

Guo, L., Riding, R., 1999. Rapid facies changes in Holocene fissure ridge hot spring travertines, Rapolano Terme, Italy. Sedimentology, 46, 1145-1158.

Hancock, P.L., Chalmers, R.M.L., Altunel, E., Cakir, Z., 1999. Travitonics: using travertines in active fault studies. J. Struct. Geol., 21, 903, 916.

IPCC, 2013. Climate Change 2013: The Physical Science Basis. Contribution of Working Group I to the Fifth Assessment Report of the Intergovernamental Panel on Climate Change [Stocker, T.F., D. Qin, G.-K. Plattner, M. Tignor, S.K. Allen, J. Boschung, A. Nauels, Y. Xia, V. Bex and P.M. Midgley (eds.)]. Cambridge University Press, Cambridge, United Kingdom and New York, NY, USA, 1535 pp.

Jolivet, L., Faccenna, C., Goffé, B., Mattei, M., Rossetti, F., Brunet, C., Storti, F., Funiciello, R., Cadet, J.P., D’Agostino, N., Parra, T., 1998. Mid crustal shear zones in postorogenic extension. Example from the northern Tyrrhenian Sea. J. Geophys. Res. 103, 12123-12160.

Jones, B., Renaut, R.W., 1995. Noncrystallographic calcite dendrites from hot-spring deposits at Lake Bogoria, Kenya. J. Sediment. Res., 65, 154-169.

Kaelin, O., Patacca, E., Renz, O., 1979. Jurassic pelagic deposits from Southeastern Tuscany; aspects of sedimentation and new biostratigraphic data. Ecoglae Geol. Helv. 72, 715-762.

Karner, D.B., Marra, F., Renne, P.R., 2001. The history of the Monti Sabatini and Alban Hills volcanoes: groundwork for assessing volcanic-tectonic hazards for Rome. J. Volcan. Geothe. Res., 107, 185-219.

Kerrick, D.M., Caldeira, K., 1993. Paleoatmospheric consequences of CO_2 released during early Cenozoic regional metamorphism in the Tethyan orogen. Chem. Geol. 108, 201-230.

Kerrick, D.M., McKibben, M.A., Seward, T.M., Caldeira, K., 1995. Convective hydrothermal CO_2 emission from high heat flow regions. Chem. Geol. 121, 285–293.

Kerrick, D.M., Caldeira, K., 1998. Metamorphic CO_2 degassing from orogenic belts. Chem. Geol., 145, 2013-232.

Kump, L.R. Brantley, S.L., Arthur, M.A., 2000. Chemical weathering, atmospheric CO_2 and climate. A. Rev. Earth Planet. Sci. 28, 611-667.

Kürschner, W.M. 2001. Leaf sensor for CO_2 in deep time. Nature, 411, 247-248.

Lasaga, A.C., Berner, R.A., Garrels, R.M., 1985. An Improved Geochemical Model of Atmospheric CO_2 Fluctuations Over the Past 100 Million Years. In: The Carbon Cycle and Atmospheric CO2: Natural Variations Archean to Present (eds E.T. Sundquist and W.S. Broecker), Geophysical Monograph Series, American Geophysical Union, Washington D.C. pp. 397-411.

Lavecchia, G., 1988. The Tyrrhenian-Apennines system: structural setting and seismotectogenesis. Tectonophysics, 147, 263-296.

La Vigna, F., Mazza, R., Capelli, G., 2013. Detecting the flow relationships between deep and shallow aquifers in an exploited groundwater system, using long-term monitoring data and quantitative hydrogeology: the Acque Albule basin case (Rome, Italy). Hydrological Processes 27, 3159-3173.

Lazzarotto, A., Aldinucci, M., Cirilli, S., Costantini, A., Decandia, F.A., Pandeli, E., Sandrelli, F., Spina, A., 2003. Stratigraphic correlation of the Upper Palaeozoic-Triassic successions in Tuscany, Italy: a review. Boll. Soc. Geol. It., vol. Spec. 1: 25–35.

Le Quéré, C., Moriarty, R., Andrew, R. M., Canadell, J. G., Sitch, S., Korsbakken, J. I., Friedlingstein, P., Peters, G. P., Andres, R. J., Boden, T. A., Houghton, R. A., House, J. I., Keeling, R. F., Tans, P., Arneth, A., Bakker, D. C. E., Barbero, L., Bopp, L., Chang, J., Chevallier, F., Chini, L. P., Ciais, P., Fader, M., Feely, R. A., Gkritzalis, T., Harris, I., Hauck, J., Ilyina, T., Jain, A. K., Kato, E., Kitidis, V., Klein Goldewijk, K., Koven, C., Landschützer, P., Lauvset, S. K., Lefèvre, N., Lenton, A., Lima, I. D., Metzl, N., Millero, F., Munro, D. R., Murata, A., Nabel, J. E. M. S., Nakaoka, S., Nojiri, Y., O'Brien, K., Olsen, A., Ono, T., Pérez, F. F., Pfeil, B., Pierrot, D., Poulter, B., Rehder, G., Rödenbeck, C., Saito, S., Schuster, U., Schwinger, J., Séférian, R., Steinhoff, T., Stocker, B. D., Sutton, A. J., Takahashi, T., Tilbrook, B., van der Laan-Luijkx, I. T., van der Werf, G. R., van Heuven, S., Vandemark, D., Viovy, N., Wiltshire, A., Zaehle, S., and Zeng, N., 2015. Global Carbon Budget 2015, Earth Syst. Sci. Data, 7, 349-396.

Liotta, D., Cernobori, L., Nicolich, R., 1998. Restricted rifting and its coexistence with compressional structures: results from the Crop03 traverse (Northern Apennines, Italy). Terra Nova 10, 16-20.

Liotta, D., Ruggieri, G., Brogi, A., Fulignati, P., Dini, A., Nardini, I., 2010. Migration of geothermal fluids in extended terranes: the ore deposits of the Boccheggiano-Montieri area (southern Tuscany, Italy). Int. Journ. Earth Sciences, 99, 623-644. DOI:10.1007/s00531-008-0411-3

Locardi, E., Nicolich, R., 2005. Crust-Mantle structures and Neogene-Quaternary magmatism in Italy. Boll. Geof. Teor. Appl. 46, 169-180.

Losacco, U., 1951. La struttura del territorio di Rapolano e Lucignano. Boll. Soc. Geol. It., 70, 402-434.

Malinverno, A., Ryan, W.B.F., 1986. Extension in the Tyrrhenian sea and shortening in the Apennines as result of arc migration driven by sinking of the lithosphere. Tectonics, 5, 227-245.

Mancini, M., Marini, M., Moscatelli, M., Pagliaroli, A., Stigliano, F., Di Salvo, C., Simionato, M., Cavinato, G.P., Corazza, A., 2014. A physical stratigraphy model for seismic microzonation of the Central Archaeological Area of Rome (Italy). Bulletin Earthquake Engineering, 12, 1339-1363.

Manfra, L., Masi, U., Turi, B., 1976. La composizione isotopica dei travertini del Lazio. Geologica Romana 15, 127-174.

Marroni, M., Molli, G., Ottria, G., Pandolfi, L., 2001. Tectono-sedimentary evolution of the External Liguride units (Northern Apennines, Italy): Insights in the pre-collisional history of a fossil ocean-continent transition zone. Geodinamica Acta 14, 307-320.

Martini, I.P., Sagri, M., 1993. Tectono-sedimentary characteristics of Late Miocene-Quaternary extensional basins of the Northern Apennines, Italy. Earth Sci. Rev. 34, 197-233.

Milli, S., Mancini, M., Moscatelli, M., Stigliano, F., Marini, M., Cavinato, G.P., 2017. From river to shelf, anatomy of a high-frequency depositional sequence: the Late Pleistocene to Holocene Tiber depositional sequence. Sedimentology, 63, 1886-1928.

Minissale, A., 2004. Origin, transport and discharge of CO_2 in central Italy. Earth Sci. Rev. 66, 89-141.

Minissale, A., Kerrick, D.M., Magro, G., Murrell, M.T., Paladini, M., Rihs, S., Sturchio, N.C., Tassi, F., Vaselli, O., 2002. Geochemistry of Quaternary travertines in the region north of Rome (Italy): structural, hydrologic and paleoclimatic implications. Earth Planet. Sci. Lett. 203, 709-728.

Molli, G., 2008. Northern Apennine–Corsica orogenic system: an updated overview. Geological Society, London, Special Publications, 298, 413-442.

Mörner, N.A., Etiope, G., 2002. Carbon degassing from the lithosphere. Global Planet. Change 33, 185-203.

Mutlu, H., Güleç, N., Hilton, D. R. 2008. Helium–carbon relationships in geothermal fluids of western Anatolia, Turkey. Chem. Geol. 247, 305-321.

Nelson, S.T., Mayo, A.L., Gilfillan, S., Dutson, S.J., Harris, R.A., Shipton, Z.K. and Tingey, D.G., 2009. Enhanced fracture permeability and accompanying fluid flow in the footwall of a normal fault: the Hurricane fault at Pah Tempe hot springs, Washington County, Utah. Geol. Soc. Am. Bull., 121, 236, 246.

Ori, G.G., Roveri, M., Vannoni, F., 1986. Plio-Pleistocene sedimentation in the Apenninnic-Adriatic foredeep (Central Adriatic Sea, Italy). In: Allen, P.A., Homewood, P. (Eds.), IAS Special Publication 8, Foreland Basins, pp. 183–198.

Pandeli, E., Bertini, G., Castellucci, P., Morelli, M., Monechi, S., 2005. The sub-Ligurian and Ligurian units of the Mt. Amiata geothermal Region (south-eastern Tuscany): new stratigraphic and tectonic data and insight into their relationships with the Tuscan Nappe. Boll. Soc. Geol. It., Vol. Spec. n.3 (2005), 55-71.

Panichi, C., Tongiorgi, E., 1975. Carbon isotopic composition of CO_2 from springs, fumaroles, mofettes and travertines of central and southern Italy: a preliminary prospection method of geothermal areas, Proc. 2nd UN Symp. On the Development and Use of Geothermal Energy, SanFrancisco, CA, 20-29 May 1975, pp. 815-825.

Parise, M., Inguscio, S., Marangella, A., 2008. Geomorfologia Carsica. Atti del 45° Corso CNSS-SSI di III livello, Grottaglie, 2-3 febbraio 2008.

Patacca, E., Sartori, R., Scandone, P., 1992. Tyrrhenian basin and Apenninic arcs: kinematic relations since late Tortonian times. Mem. Soc. Geol. It., 45, 425-451.

Pazzaglia, F., R. Barchi, M., Buratti, N., Cherin, M., Pandolfi, L., Ricci, M., 2013. Pleistocene Calcareous Tufa from the Ellera Basin (Umbria, Central Italy) as a key for an integrated Paleoenvironmental and Tectonic Reconstruction. Quaternary International, 292, 59-70. DOI: 10.1016/j.quaint.2012.11.020

Peccerillo, A., 2003. Plio-Quaternary magmatism in Italy. Episodes, 26, 222-226.

Peccerillo, A., 2005. Plio-Quaternary volcanism in Italy. Petrology, geochemistry, geodynamics. Springer, Heidelberg, 365 pp.

Pedley, M., 2009. Tufas and travertines of the Mediterranean region: a testing ground for freshwater carbonate concepts and developments. Sedimentology, 56, 221, 246.

Pentecost, A., Tortora, C., 1989. Bagni di Tivoli, Lazio: a modern travertine depositing site and its associated microorganisms. Boll. Soc. Geol. It., 108, 315–324.

Pentecost, A., 2005. Travertine. Springer, Berlin Heidelberg, 445 pp.

Rainey, D.K., Jones, B., 2009. Abiotic versus biotic controls on the development of the Fairmont Hot Springs carbonate deposit, British Columbia, Canada. Sedimentology, 56, 1832-1857.

Regnier, P., Friedlingstein, P., Ciais, P., Mackenzie, F.T., Gruber, N., Janssens, I.A., Laruelle, G.G., Lauerwald, R., Luyssaert, S., Andersson, A.J., Arndt, S.,Arnosti, C., Borges, A.V.,Dale, A.W., Gallego-Sala, A., Goddéris, Y., Goossens, N., Hartmann, J., Heinze, C., Ilyina, T., Joos, F., LaRowe, D.E., Leifeld, J.,Meysman, F.J.R., Munhoven,G., Raymond, P.A., Spahni, R., Suntharalingam, P., Thullner, M., 2013. Anthropogenic perturbation of the carbon fluxes from land to ocean. Nature Geoscience 6, 597–607.

Radtke, U., Hausmann, R., Hentzsch, B., 1986. The travertine complex of Vulci (Central Italy). An indicator of Quaternary climatic change. Proceedings of a Symposium on Climatic Fluctuations during the Quaternary in the Western Mediterranean, 2, 273-292.

Ricci Lucchi, F., 1986. Oligocene to Recent foreland basins Northern Apennines. I.A.S., Special Public. No.8, Blackwell, 105-139.

Rogie, J. D., Kerrick, D. M., Chiodini, G., Frondini, F. 2000. Flux measurements of nonvolcanic CO_2 emission from some vents in central Italy. J. Geophys. Res. Solid Earth 105(B4), 8435-8445.

Ronchi, P., Cruciani, F., 2015. Continental carbonates as a hydrocarbon reservoir, an analog case study from the travertine of Saturnia, Italy. AAPG Bulletin, 99, 4, 711-734.

Rossetti, F., Faccenna, C., Jolivet, L., Funiciello, R., Tecce, F., Brunet, C., 1999. Syn-versus post-orogenic extension: the case study of Giglio Island (Northern Tyrrhenian Sea, Italy). Tectonophysics 304, 71-93.

Rossetti, F., Faccenna, C., Jolivet, L., Goffe, B., Funiciello, R., 2002. Structural signature and exhumation PTt paths of the blueschist units exposed in the interior of the Northern Apennine chain, tectonic implications. Boll. Soc. Geol. It. 121, 829-842.

Rossetti, F., Glodny, J., Theye, T., Maggi, M., 2015. Pressure–temperature–deformation–time of the ductile Alpine shearing in Corsica: from orogenic construction to collapse. Lithos, 218-219, 99-116.

Rowland, J.V., Sibson, R.H., 2004. Structural controls on hydrothermal flow in a segmented rift system, Taupo Volcanic Zone, New Zealand. Geofluids, 4, 259-283.

Scott, M., Lindsey, R., 2016. Which emits more carbon dioxide: volcanoes or human activities? NOAA, 2016. Climate.gov. website: https://www.climate.gov/news-features/climate-qa/which-emitsmore-carbon-dioxide-volcanoes-or-human-activities.

Serri, G., Innocenti, F., Manetti, P., 1993. Geochemical and petrological evidence of the subduction of delaminated Adriatic continental lithosphere in the genesis of the Neogene–Quaternary magmatism of Central Italy. Tectonophysics, 223, 117-147.

Soete, J., Kleipool, L., Claes, H., Claes, S., Hamaekers, H., Kele S., Özkul, M., Foubert, A., Reijmer, J., Swennen, R., 2015. Acoustic properties in travertines and their relation to porosity and pore types. Marine and Petroleum Geology, 59, 320-335.

Soligo, M., Tuccimei, P., Barberi, R., Delitala, M.C., Miccadei, E., Taddeucci, A., 2002. U/Th dating of freshwater travertine from Middle Velino Valley (Central Italy): paleoclimatic and geological implications. Palaeogeography, Palaeoclimatology, Palaeoecology, 184, 147-161.

Taddeucci, A., Voltaggio, M., 1987. Th-230 dating of the travertines connected to the Vulsini Mts. Volcanism (Northern Latium, Italy): neotectonics and hydrogeology. Per. Miner., 56, 295-302.

Török, Á., Mindszenty, A., Claes, H., Kele, S., Fodor, L., Swennen, R., 2017. Geobody architecture of continental carbonates: "Gazda" travertine quarry (Süttő, Gerecse Hills, Hungary). Quaternary International, 437 (Part A), 164-185.

Vignaroli, G., Pinton, A., De Benedetti, A.A., Giordano, G., Rossetti, F., Soligo, M., Berardi, G., 2013. Structural compartmentalisation of a geothermal system, the Torre Alfina field (central Italy). Tectonophysics, 608, 482–498.

Vignaroli, G., Berardi, G., Billi, A., Kele, S., Rossetti, F., Soligo, M., Bernasconi, S.M., 2016. Tectonics, hydrothermalism, and paleoclimate recorded by Quaternary travertines and their spatio-temporal distribution in the Albegna basin, central Italy: Insights on Tyrrhenian margin neotectonics. Lithosphere 8, 335-358.

Zucchi, M., Brogi, A., Liotta, D., Rimondi, V., Ruggieri, G., Montegrossi, G., Caggianelli, A., Dini, A. 2017. Permeability and hydraulic conductivity of faulted micaschist in the eastern Elba Island exhumed geothermal system (Tyrrhenian sea, Italy): insights from Cala Stagnone. Geothermics 70, 125-145.

Figure caption

Fig. 1. Geological map of Central Italy and location of study areas. Red circles indicate present-day geothermal systems and blue circles indicate CO_2-rich springs. Purple stars indicate the three study areas, i.e. from N to S, Rapolano, Canino and Tivoli (redrawn and modified after De Rita et al. 1995, 2002; Gaeta et al. 2000; Karner et al. 2001; Minissale, 2004; Della Porta et al., 2017).

Fig. 2. Aerial view of the three study areas (images modified from Google Earth/Maps; Digital Globe 2018): A) Rapolano; B) Canino; C) Tivoli. For each area the isopachs of the travertine deposits are shown as well as the rivers and main springs. Alongside are shown the geological maps of the three study areas. The Meso-Cenozoic limestones generally represent the major fractured aquifers hosting deep CO_2 rich fluids. Faults and open fractures represent the zone where deep fluids can reach the surface, generating the thermal springs depositing travertines (modified after Chiodini et al., 1991; Faccena et al., 2008; Brogi and Capezzuoli, 2009; Della Porta et al., 2017).

Fig. 3. 3D reconstructions of the volume occupied by the travertine deposits: A) Rapolano Terme; B) Canino; C) Tivoli. The limits and the isopachs of the travertine deposits have been used to reconstruct the 3D models. The different colors indicate the thicknesses of the deposits. The different morphologies highlight the presence of paleo-valleys and depressions filled during travertine deposition.

Fig. 4. Histograms of (a) porosity and (b) $CaCO_3$ content.

Fig. 5. Log F-CO2 vs logarithm of the recharge area. Along with the CO_2 discharge rate of Rapolano, Canino and Tivoli travertine systems, in the diagram are shown (a) CO_2 discharge rates of adjacent main geothermal fields of the study area (red circles - Gambardella et al., 2004) and (b)

the CO_2 discharge rates of some large, CO_2 rich, springs or groups of springs (blue circles - Chiodini et al., 1999 & 2000; Chiodini and Frondini, 2001; Frondini 2008; Frondini et al., 2012). The solid line represents the global baseline of CO_2 fluxes from high heat flow regions (Kerrick et al., 1995) and the dashed lines indicate the range of variation of □CO_2 in western central Italy (Chiodini et al., 2000).

Fig. 6. Travertine deposits dating by $^{234}U/^{230}Th$ and ^{14}C in western central Italy.

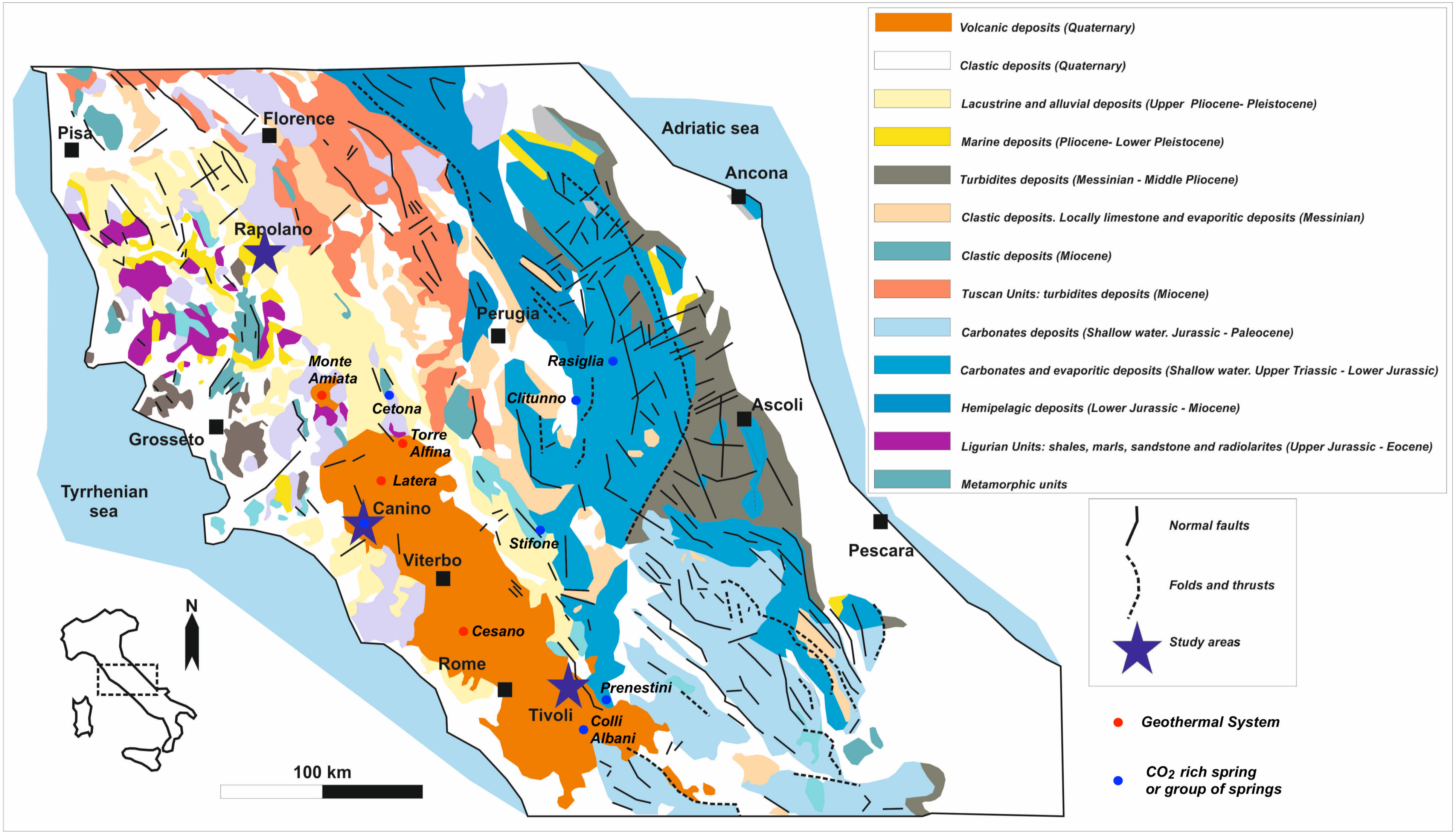
Volcanic deposits (Quaternary)
Clastic deposits (Quaternary)
Lacustrine and alluvial deposits (Upper Pliocene- Pleistocene)
Marine deposits (Pliocene- Lower Pleistocene)
Turbidites deposits (Messinian - Middle Pliocene)
Clastic deposits. Locally limestone and evaporitic deposits (Messinian)
Clastic deposits (Miocene)
Tuscan Units: turbidites deposits (Miocene)
Carbonates deposits (Shallow water. Jurassic - Paleocene)
Carbonates and evaporitic deposits (Shallow water. Upper Triassic - Lower Jurassic)
Hemipelagic deposits (Lower Jurassic - Miocene)
Ligurian Units: shales, marls, sandstone and radiolarites (Upper Jurassic - Eocene)
Metamorphic units
Normal faults
Folds and thrusts
Study areas
Geothermal System
CO_2 rich spring
or group of springs
Pisa
Florence
Adriatic sea
Ancona
Rapolano
Perugia
Rasiglia
Monte
Amiata
Cetona
Clitunno
Ascoli
Grosseto
Torre
Alfina
Latera
Tyrrhenian
sea
Canino
Stifone
Pescara
Viterbo
Cesano
Rome
Prenestini
Tivoli
Colli
Albani
N
100 km

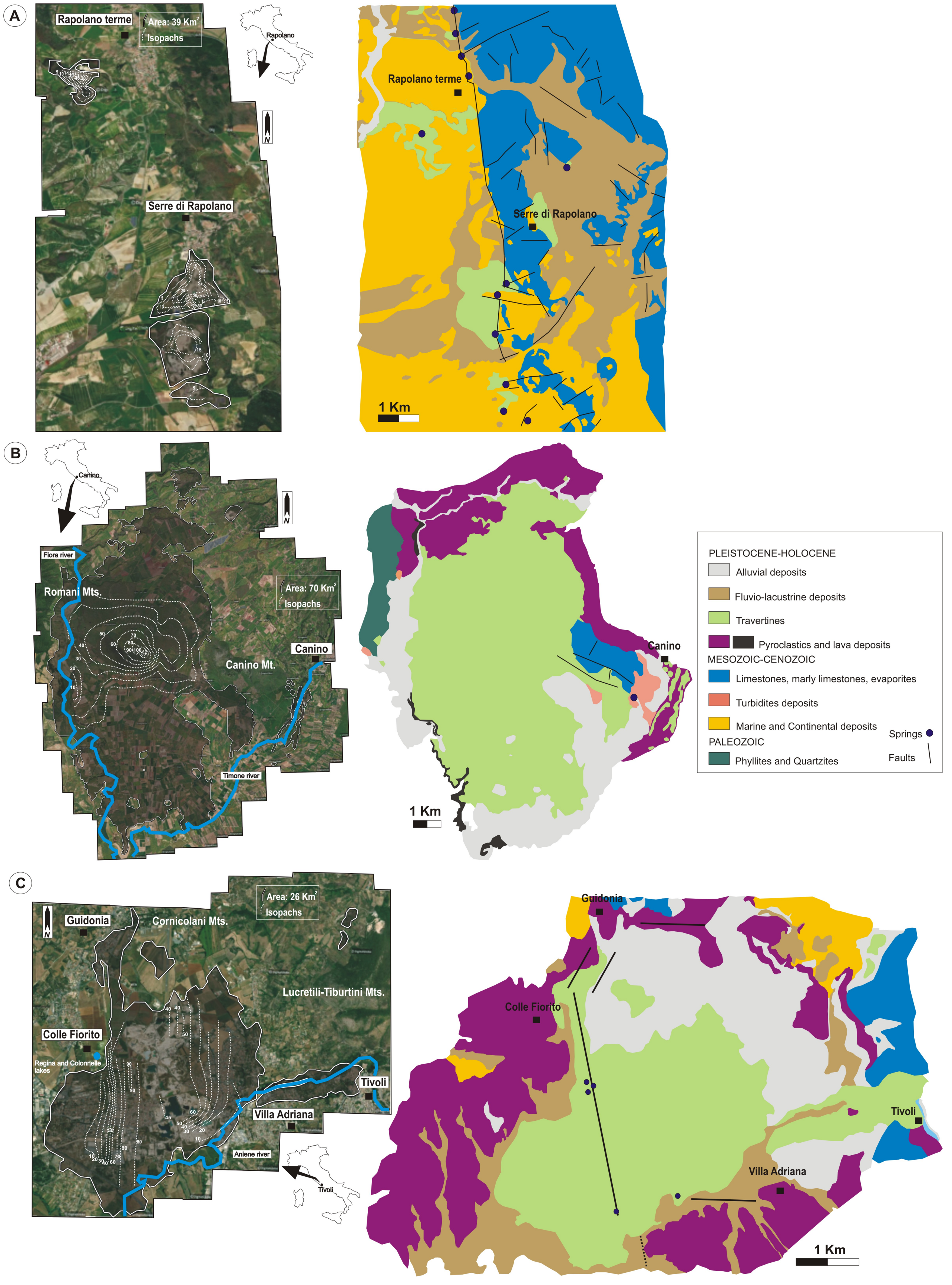
A
Rapolano terme
Area: 39 Km2
Isopachs
Rapolano
Serre di Rapolano
Rapolano terme
Serre di Rapolano
1 Km
B
Canino
Fiora river
Romani Mts.
Area: 70 Km2
Isopachs
Canino
Canino Mt.
Timone river
Canino
1 Km
PLEISTOCENE-HOLOCENE
Alluvial deposits
Fluvio-lacustrine deposits
Travertines
Pyroclastics and lava deposits
MESOZOIC-CENOZOIC
Limestones, marly limestones, evaporites
Turbidites deposits
Marine and Continental deposits
PALEOZOIC
Phyllites and Quartzites
Springs
Faults
C
Area: 26 Km2
Isopachs
Guidonia
Cornicolani Mts.
Lucretili-Tiburtini Mts.
Colle Fiorito
Regina and Colonnelle lakes
Tivoli
Villa Adriana
Aniene river
Tivoli
Guidonia
Colle Fiorito
Tivoli
Villa Adriana
1 Km

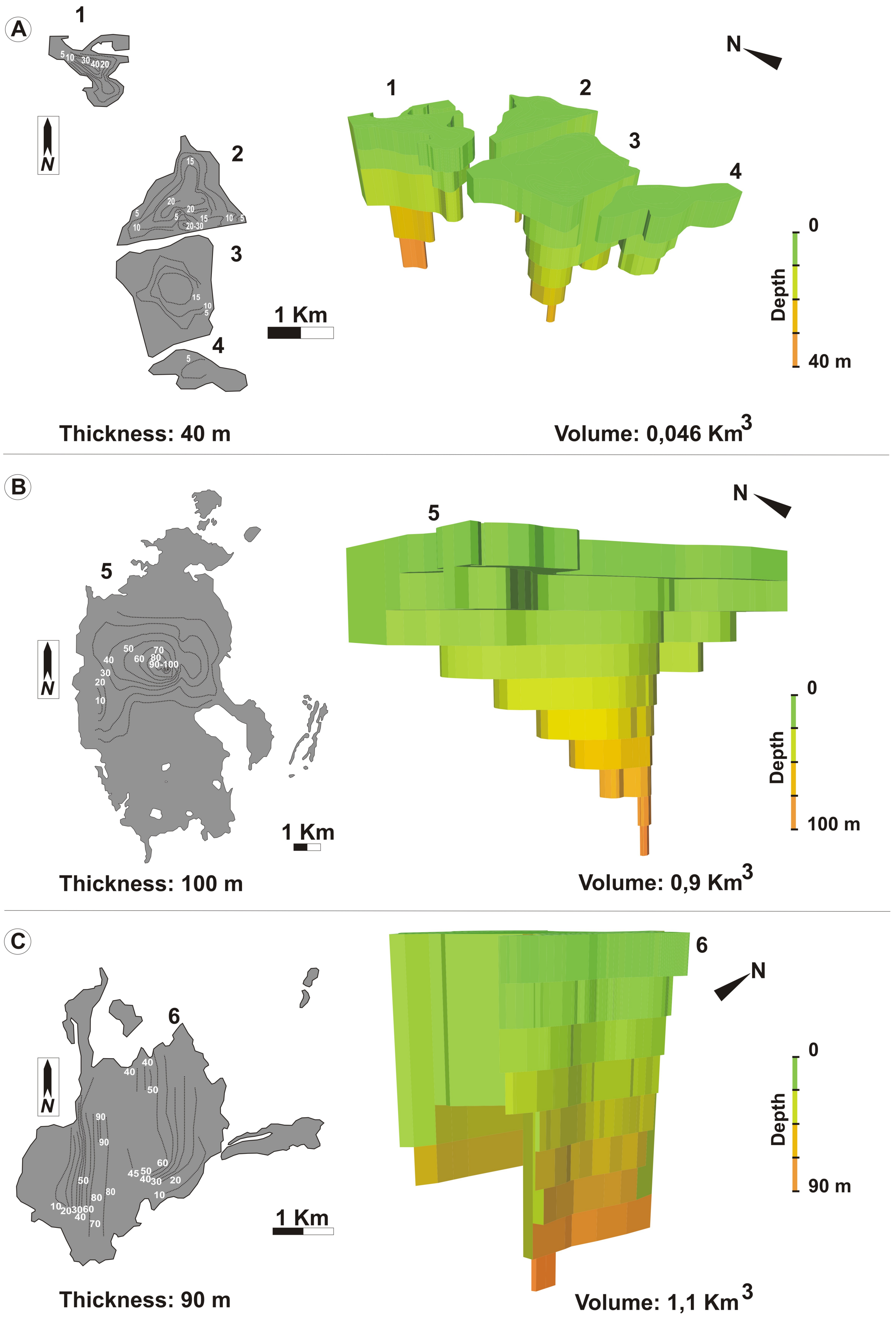

A
1
2
3
4
N
1 Km
Depth
0
40 m
Thickness: 40 m
Volume: 0,046 Km3
B
5
N
1 Km
Depth
0
100 m
Thickness: 100 m
Volume: 0,9 Km3
C
6
N
1 Km
Depth
0
90 m
Thickness: 90 m
Volume: 1,1 Km3

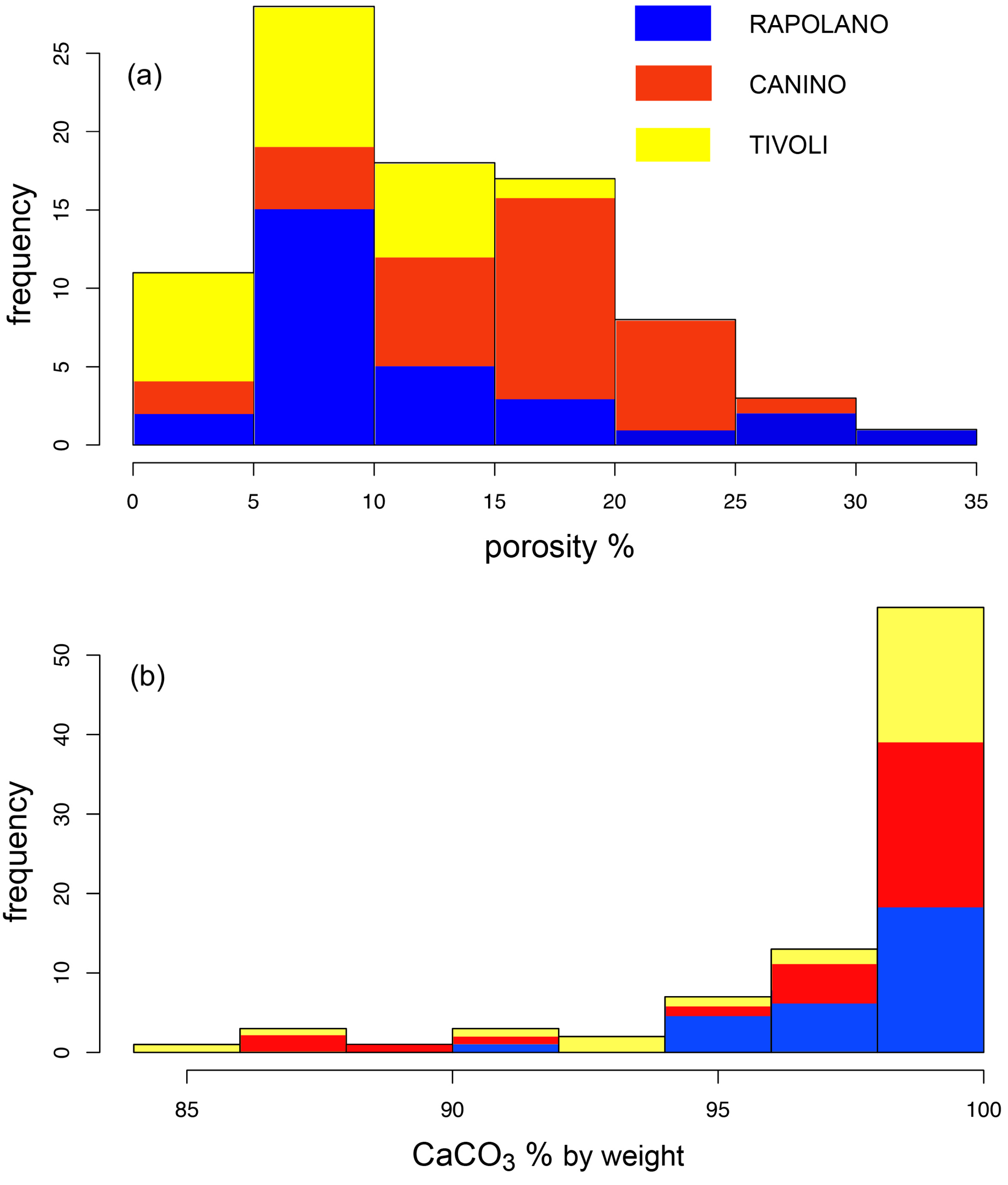

(a)
RAPOLANO
CANINO
TIVOLI
frequency
0
5
10
15
20
25
0
5
10
15
20
25
30
35
porosity %
(b)
frequency
0
10
20
30
40
50
85
90
95
100
CaCO3 % by weight

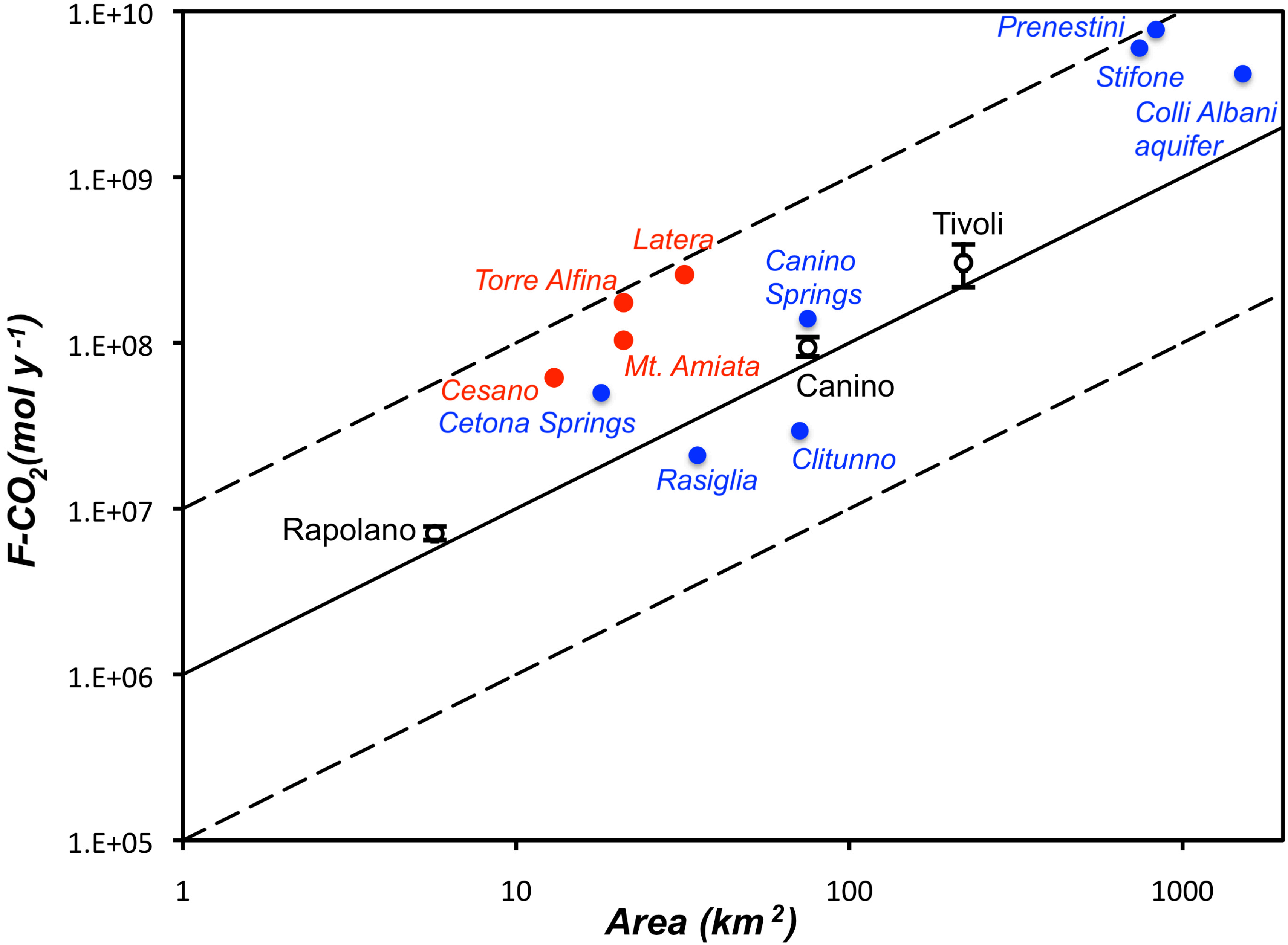

1.E+10
1.E+09
1.E+08
1.E+07
1.E+06
1.E+05
F-CO2(mol y-1)
1
10
100
1000
Area (km 2)
Prenestini
Stifone
Colli Albani
aquifer
Tivoli
Latera
Torre Alfina
Canino
Springs
Mt. Amiata
Canino
Cesano
Cetona Springs
Clitunno
Rasiglia
Rapolano

Travertine deposits	Authors	U/Th Age (Ka)	^{14}C Age (years B.P.)
- *Umbria-Marche Appenine*	Calderoni et al., (1996)		From 8.260 ± 100
- *Sarteano*	Brogi et al., (2012)	From 268 ± 22	
- *Rapolano Campo Muri quarry*	Carrara et al., (1998)	From 24 ± 3.0	
- *Rapolano Terme Oliviera quarry*	Brogi et al., (2010)	From 157 ± 15	
- *Bagni San Filippo*	Minissale & Sturchio, 2004	From 55	
- *Pescara valley (Abruzzo)*	Carrara, (1998)	From 120 ± 12	
- *Rocchetta al Volturno*	Brancaccio et al., (1998)	From 75 ± 8	
- *Valdelsa*	Capezzuoli et al., (2010)	From 114.3 ± 5.2	
- *Aniene valley (Latium)*	Carrara et al., (2006)	From 112 ± 7	
- *Velino valley (Latium)*	Soligo et al., (2002)	From 113.6 ± 18	
- *Tuscia (Latium)*	Taddeucci & Voltaggio, (1987)	From 281 ± 39	
- *Ellera Basin (Umbria)*	Pazzaglia et al., (2011)	From 115 ± 8	

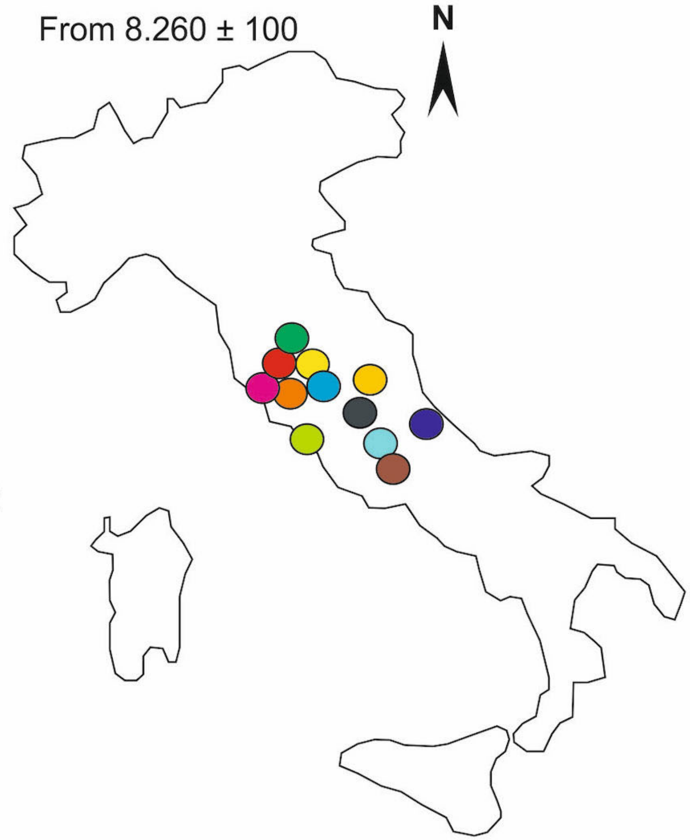

Table 1. Central tendency and variability of porosity and $CaCO_3$ content obtained from dissolution analysis. For each variable are reported: the mean, the standard deviation, the median, the mean absolute deviation from median (MAD) and the interquartile range (IQR)

	Rapolano	Canino	Tivoli	All samples
observations	29	34	23	86
porosity (%)				
mean	11.39	15.93	7.48	12.14
std	7.23	5.84	4.01	6.75
median	8.45	16.78	9.05	10.68
MAD	2.96	4.42	3.34	4.96
IQR	6.90	5.94	6.53	10.21
$CaCO_3$ (%)				
mean	97.71	96.90	98.06	97.44
std	2.13	4.11	3.46	3.39
median	98.34	99.09	99.29	99.09
MAD	1.58	2.64	1.64	2.06
IQR	2.71	3.26	1.19	2.89

Table 2. Carbon dioxide flux calculations

	Rapolano	Canino	Tivoli
travertine volume (km^3)	0.046	0.90	1.10
recharge area (km^2)	5.7	75	220
$CaCO_3$ (moles $x10^{12}$)	1.11± 0.02	19.60 ± 0.52	26.49 ± 0.69
Age (ka)	157 ± 15	209 ± 28	87 ± 24
F-CO_2 (mol y^{-1} $x10^6$)	7.1±1.1	93.8±12.8	304.5±88.9
f-CO_2 (mol y^{-1} km^{-2} x 10^6)	1.24±0.12	1.25±0.18	1.38±0.42

Individual contribution to the paper

Alessandro Mancini: Conceptualization, Methodology, Software, Investigation, Writing- Original draft preparation. **Francesco Frondini**: Conceptualization, Methodology, Formal Analysis, Supervision, Writing- Original draft preparation. **Enrico Capezzuoli**: Conceptualization, Investigation, Writing- Original draft preparation. **Eduard Galvez Mejia**: Investigation. **Gabriele Lezzi**: Investigation. **David Matarazzi**: Investigation. **Andrea Brogi**: Writing- Original draft preparation. **Rudy Swennen**: Conceptualization, Writing- Original draft preparation.

SUPPLEMENTARY MATERIAL 1: samples and stratigraphic logs

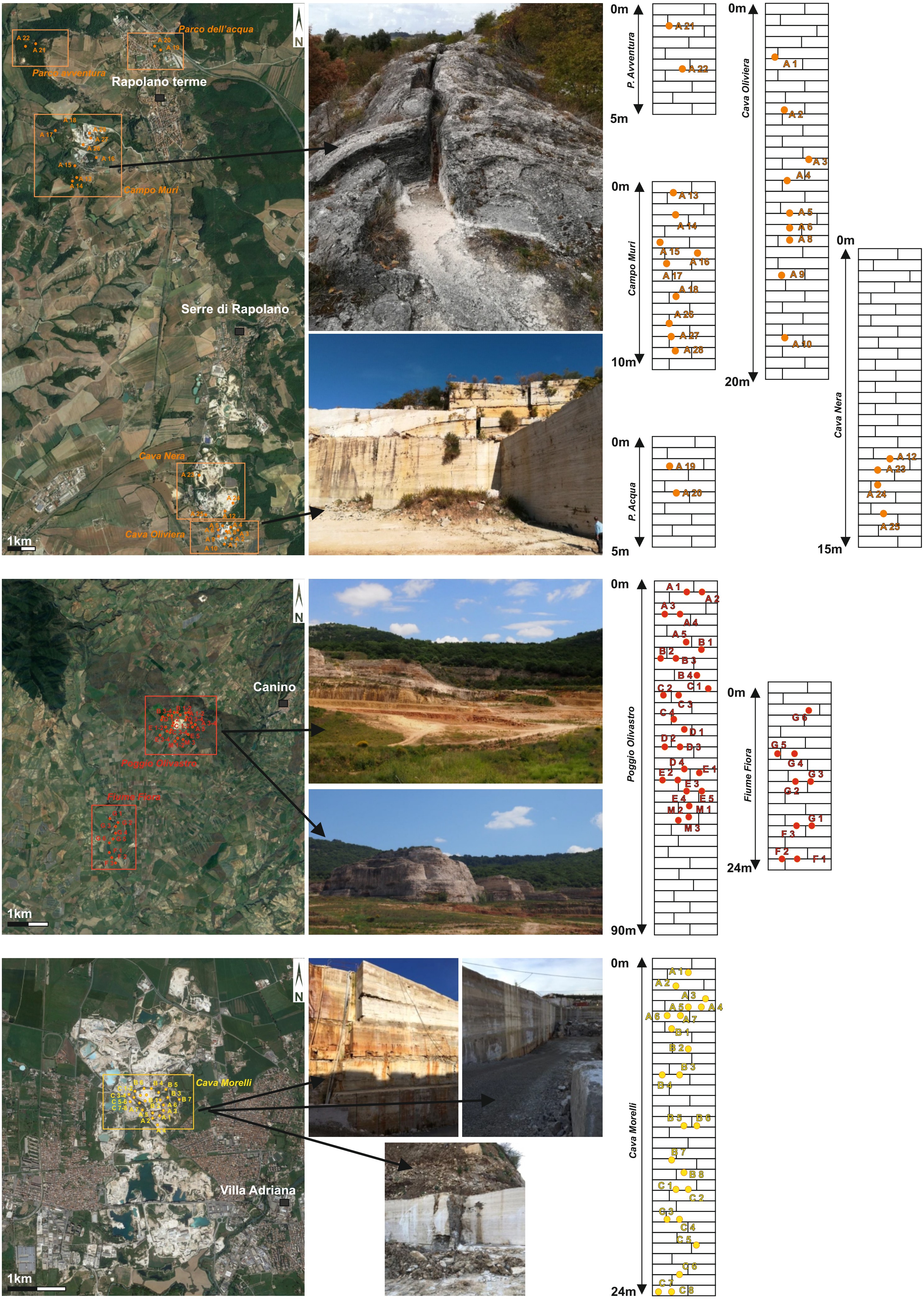

SUPPLEMENTARY MATERIAL 2: Mass, volume of travertine specimens and results of dissolution experiments

System	Section	ID	W_i g	V cm^3	ρ_b g/cm^3	W_r g	$CaCO_3$ g	Porosity fraction	Porosity %	$CaCO_3$ %	$CaCO_3$ fraction
Rapolano	Cava Oliviera	A1	34.266	13.50	2.54	0.63	33.64	0.06	5.99	98.17	0.982
Rapolano	Cava Oliviera	A2	28.911	15.00	1.93	0.80	28.11	0.29	28.61	97.23	0.972
Rapolano	Cava Oliviera	A3	26.749	10.50	2.55	0.16	26.59	0.06	5.65	99.42	0.994
Rapolano	Cava Oliviera	A4	31.028	12.50	2.48	0.09	30.94	0.08	8.07	99.72	0.997
Rapolano	Cava Oliviera	A5	29.538	11.50	2.57	0.09	29.45	0.05	4.87	99.71	0.997
Rapolano	Cava Oliviera	A6	23.396	9.50	2.46	2.25	21.15	0.09	8.79	90.39	0.904
Rapolano	Cava Oliviera	A8	36.459	15.50	2.35	2.07	34.39	0.13	12.88	94.33	0.943
Rapolano	Cava Oliviera	A9	31.731	12.50	2.54	0.58	31.15	0.06	5.98	98.16	0.982
Rapolano	Cava Oliviera	A10	33.103	16.50	2.01	0.43	32.68	0.26	25.69	98.71	0.987
Rapolano	Cava Nera	A12	24.665	9.50	2.60	0.63	24.04	0.04	3.84	97.45	0.974
Rapolano	Campo Muri	A13	20.355	8.50	2.39	0.19	20.17	0.11	11.31	99.09	0.991
Rapolano	Campo Muri	A14	36.914	15.50	2.38	1.08	35.84	0.12	11.79	97.09	0.971
Rapolano	Campo Muri	A15	22.336	10.00	2.23	0.26	22.08	0.17	17.27	98.86	0.989
Rapolano	Campo Muri	A16	20.474	9.00	2.27	0.15	20.33	0.16	15.74	99.29	0.993
Rapolano	Campo Muri	A17	14.037	7.50	1.87	0.12	13.92	0.31	30.68	99.16	0.992
Rapolano	Campo Muri	A18	22.044	10.50	2.10	0.92	21.13	0.22	22.24	95.85	0.958
Rapolano	Parco dell'Acqua	A19	23.482	9.50	2.47	1.23	22.25	0.08	8.45	94.76	0.948
Rapolano	Parco dell'Acqua	A20	36.606	14.50	2.52	0.56	36.05	0.06	6.50	98.48	0.985
Rapolano	Parco Avventura	A21	32.006	12.50	2.56	0.20	31.81	0.05	5.17	99.39	0.994
Rapolano	Parco Avventura	A22	30.273	12.50	2.42	1.59	28.68	0.10	10.30	94.75	0.948
Rapolano	Cava Dei	A23	28.426	11.50	2.47	0.95	27.48	0.08	8.45	96.68	0.967
Rapolano	Cava Nera	A24	31.896	12.50	2.55	0.17	31.73	0.05	5.49	99.48	0.995
Rapolano	Cava Nera	A25	29.407	11.50	2.56	0.49	28.92	0.05	5.29	98.34	0.983
Rapolano	Campo Muri	A26a	43.385	17.50	2.48	1.78	41.61	0.08	8.18	95.91	0.959
Rapolano	Campo Muri	A26b	27.226	11.00	2.48	0.76	26.46	0.08	8.33	97.20	0.972
Rapolano	Campo Muri	A27a	19.947	8.00	2.49	0.06	19.89	0.08	7.65	99.71	0.997
Rapolano	Campo Muri	A27b	16.581	7.00	2.37	0.55	16.04	0.12	12.27	96.71	0.967
Rapolano	Campo Muri	A28a	29.378	12.00	2.45	0.06	29.32	0.09	9.33	99.79	0.998
Rapolano	Campo Muri	A28b	31.950	14.00	2.28	0.08	31.87	0.15	15.48	99.75	0.997
Canino	Poggio Olivastro A	A-1	16.260	8.00	2.03	0.08	16.18	0.25	24.72	99.53	0.995
Canino	Poggio Olivastro A	A-2	26.870	12.80	2.10	0.25	26.62	0.22	22.25	99.08	0.991
Canino	Poggio Olivastro A	A-3	15.930	7.50	2.12	0.06	15.87	0.21	21.33	99.64	0.996
Canino	Poggio Olivastro A	A-4	18.920	9.00	2.10	0.04	18.88	0.22	22.14	99.80	0.998
Canino	Poggio Olivastro A	A-5	19.250	9.00	2.14	0.02	19.23	0.21	20.78	99.91	0.999
Canino	Poggio Olivastro B	B-1	13.240	7.00	1.89	0.11	13.13	0.30	29.95	99.19	0.992
Canino	Poggio Olivastro B	B-2	18.020	8.00	2.25	0.29	17.73	0.17	16.57	98.41	0.984
Canino	Poggio Olivastro B	B-3	21.940	10.00	2.19	0.34	21.60	0.19	18.74	98.46	0.985
Canino	Poggio Olivastro B	B-4	15.690	7.00	2.24	0.10	15.59	0.17	16.98	99.38	0.994
Canino	Poggio Olivastro M	M-1	20.110	8.00	2.51	2.57	17.54	0.07	6.90	87.24	0.872
Canino	Poggio Olivastro M	M-2	18.480	7.00	2.64	0.17	18.31	0.02	2.22	99.10	0.991
Canino	Poggio Olivastro M	M-3	18.070	8.00	2.26	0.43	17.64	0.16	16.34	97.64	0.976
Canino	Poggio Olivastro C	C-1	18.820	9.00	2.09	0.04	18.78	0.23	22.55	99.80	0.998
Canino	Poggio Olivastro C	C-2	25.010	11.00	2.27	0.08	24.93	0.16	15.79	99.69	0.997
Canino	Poggio Olivastro C	C-3	25.500	11.00	2.32	0.54	24.96	0.14	14.14	97.89	0.979
Canino	Poggio Olivastro C	C-4	19.100	9.00	2.12	0.09	19.01	0.21	21.40	99.54	0.995
Canino	Poggio Olivastro D	D-1	33.180	13.50	2.46	0.23	32.95	0.09	8.97	99.32	0.993
Canino	Poggio Olivastro D	D-2	17.230	7.50	2.30	0.11	17.12	0.15	14.91	99.38	0.994
Canino	Poggio Olivastro D	D-3	22.200	10.00	2.22	0.20	22.00	0.18	17.78	99.11	0.991
Canino	Poggio Olivastro D	D-4	20.590	8.00	2.57	0.11	20.48	0.05	4.68	99.48	0.995
Canino	Poggio Olivastro E	E-1	25.150	10.00	2.52	0.10	25.05	0.07	6.85	99.61	0.996
Canino	Poggio Olivastro E	E-2	20.490	9.00	2.28	0.45	20.04	0.16	15.68	97.82	0.978
Canino	Poggio Olivastro E	E-3	26.500	12.00	2.21	0.26	26.24	0.18	18.21	99.03	0.990
Canino	Poggio Olivastro E	E-4	18.420	8.00	2.30	0.05	18.37	0.15	14.72	99.74	0.997
Canino	Poggio Olivastro E	E-5	20.110	9.00	2.23	0.02	20.09	0.17	17.24	99.92	0.999
Canino	Fiume Fiora F	F-1	16.610	7.50	2.21	0.89	15.72	0.18	17.98	94.66	0.947
Canino	Fiume Fiora F	F-2	21.920	10.00	2.19	1.68	20.24	0.19	18.81	92.35	0.923
Canino	Fiume Fiora F	F-3	20.840	9.00	2.32	2.68	18.16	0.14	14.24	87.15	0.872
Canino	Fiume Fiora G	G-1	17.880	8.00	2.24	2.05	15.83	0.17	17.22	88.55	0.886
Canino	Fiume Fiora G	G-2	20.420	8.50	2.40	0.70	19.72	0.11	11.02	96.59	0.966
Canino	Fiume Fiora G	G-3	34.320	14.00	2.45	1.28	33.04	0.09	9.21	96.28	0.963
Canino	Fiume Fiora G	G-4	26.580	12.00	2.22	3.27	23.31	0.18	17.96	87.71	0.877
Canino	Fiume Fiora G	G-5	21.680	9.00	2.41	2.03	19.65	0.11	10.78	90.65	0.907
Canino	Fiume Fiora G	G-6	28.230	12.00	2.35	1.98	26.25	0.13	12.87	93.00	0.930
Tivoli	Cava Morelli 3° banco	A1	23.196	9.50	2.44	0.16	23.03	0.10	9.57	99.29	0.993
Tivoli	Cava Morelli 3° banco	A2	23.170	9.50	2.44	0.14	23.03	0.10	9.67	99.40	0.994
Tivoli	Cava Morelli 3° banco	A3	19.637	8.00	2.45	0.01	19.63	0.09	9.09	99.94	0.999
Tivoli	Cava Morelli 3° banco	A4	22.424	8.50	2.64	0.23	22.19	0.02	2.29	98.96	0.990
Tivoli	Cava Morelli 3° banco	A5	31.384	12.50	2.51	0.03	31.36	0.07	7.01	99.91	0.999
Tivoli	Cava Morelli 3° banco	A6	25.324	10.50	2.41	0.05	25.28	0.11	10.67	99.81	0.998
Tivoli	Cava Morelli 3° banco	A7	25.515	10.50	2.43	0.02	25.49	0.10	10.00	99.91	0.999

Tivoli	Cava Morelli 2° banco	B1	24.749	10.50	2.36	2.40	22.35	0.13	12.70	90.30	0.903
Tivoli	Cava Morelli 2° banco	B2	24.326	9.50	2.56	0.03	24.30	0.05	5.16	99.88	0.999
Tivoli	Cava Morelli 2° banco	B3	27.541	10.50	2.62	3.96	23.59	0.03	2.85	85.64	0.856
Tivoli	Cava Morelli 2° banco	B4	26.924	10.50	2.56	0.37	26.55	0.05	5.03	98.61	0.986
Tivoli	Cava Morelli 2° banco	B5	24.490	9.50	2.58	0.60	23.89	0.05	4.52	97.56	0.976
Tivoli	Cava Morelli 2° banco	B6	21.375	9.50	2.25	0.04	21.33	0.17	16.67	99.80	0.998
Tivoli	Cava Morelli 2° banco	B7	31.068	13.00	2.39	1.52	29.55	0.11	11.49	95.10	0.951
Tivoli	Cava Morelli 2° banco	B8	25.447	10.50	2.42	0.17	25.28	0.10	10.24	99.32	0.993
Tivoli	Cava Morelli 1° banco	C1	26.529	11.00	2.41	0.24	26.29	0.11	10.68	99.11	0.991
Tivoli	Cava Morelli 1° banco	C2	23.329	9.50	2.46	0.09	23.24	0.09	9.05	99.60	0.996
Tivoli	Cava Morelli 1° banco	C3	27.397	11.00	2.49	0.11	27.29	0.08	7.75	99.60	0.996
Tivoli	Cava Morelli 1° banco	C4	29.619	11.00	2.69	1.06	28.56	0.00	0.27	96.43	0.964
Tivoli	Cava Morelli 1° banco	C5	26.962	11.00	2.45	0.08	26.88	0.09	9.22	99.71	0.997
Tivoli	Cava Morelli 1° banco	C6	24.698	9.50	2.60	0.18	24.52	0.04	3.71	99.28	0.993
Tivoli	Cava Morelli 1° banco	C7	26.357	10.00	2.64	0.24	26.11	0.02	2.38	99.07	0.991
Tivoli	Cava Morelli 1° banco	C8	26.403	10.00	2.64	0.22	26.18	0.02	2.21	99.15	0.992